



OPEN ACCESS

EDITED BY

John Albeck,
University of California, Davis,
United States

REVIEWED BY

Michelle Mendoza,
The University of Utah, United States
Nan Hao,
University of California, San Diego,
United States

*CORRESPONDENCE

Gregor Neuert,
✉ gregor.neuert@vanderbilt.edu

SPECIALTY SECTION

This article was submitted
to Signaling, a section of the
journal Frontiers in Cell and
Developmental Biology

RECEIVED 15 December 2022

ACCEPTED 08 March 2023

PUBLISHED 21 March 2023

CITATION

Thiemicke A and Neuert G (2023), Rate
thresholds in cell signaling have
functional and phenotypic consequences
in non-linear time-
dependent environments.
Front. Cell Dev. Biol. 11:1124874.
doi: 10.3389/fcell.2023.1124874

COPYRIGHT

© 2023 Thiemicke and Neuert. This is an
open-access article distributed under the
terms of the [Creative Commons
Attribution License \(CC BY\)](https://creativecommons.org/licenses/by/4.0/). The use,
distribution or reproduction in other
forums is permitted, provided the original
author(s) and the copyright owner(s) are
credited and that the original publication
in this journal is cited, in accordance with
accepted academic practice. No use,
distribution or reproduction is permitted
which does not comply with these terms.

Rate thresholds in cell signaling have functional and phenotypic consequences in non-linear time-dependent environments

Alexander Thiemicke^{1,2} and Gregor Neuert^{1,2,3,4*}

¹Department of Molecular Physiology and Biophysics, School of Medicine, Vanderbilt University, Nashville, TN, United States, ²Program in Chemical and Physical Biology, Vanderbilt University, Nashville, TN, United States, ³Department of Biomedical Engineering, School of Engineering, Vanderbilt University, Nashville, TN, United States, ⁴Department of Pharmacology, School of Medicine, Vanderbilt University, Nashville, TN, United States

All cells employ signal transduction pathways to respond to physiologically relevant extracellular cytokines, stressors, nutrient levels, hormones, morphogens, and other stimuli that vary in concentration and rate in healthy and diseased states. A central unsolved fundamental question in cell signaling is whether and how cells sense and integrate information conveyed by changes in the rate of extracellular stimuli concentrations, in addition to the absolute difference in concentration. We propose that different environmental changes over time influence cell behavior in addition to different signaling molecules or different genetic backgrounds. However, most current biomedical research focuses on acute environmental changes and does not consider how cells respond to environments that change slowly over time. As an example of such environmental change, we review cell sensitivity to environmental rate changes, including the novel mechanism of rate threshold. A rate threshold is defined as a threshold in the rate of change in the environment in which a rate value below the threshold does not activate signaling and a rate value above the threshold leads to signal activation. We reviewed p38/Hog1 osmotic stress signaling in yeast, chemotaxis and stress response in bacteria, cyclic adenosine monophosphate signaling in Amoebae, growth factors signaling in mammalian cells, morphogen dynamics during development, temporal dynamics of glucose and insulin signaling, and spatio-temporal stressors in the kidney. These reviewed examples from the literature indicate that rate thresholds are widespread and an underappreciated fundamental property of cell signaling. Finally, by studying cells in non-linear environments, we outline future directions to understand cell physiology better in normal and pathophysiological conditions.

KEYWORDS

cell signaling, quantitative biology, single cell, time lapse microscopy, dynamic environments, flow cytometry, rate threshold, systems biology

1 Introduction

All living cells sense and respond to environmental changes (Lim et al., 2014; Alberts et al., 2015; Murugan et al., 2021). Concentrations of physiologically relevant external stimuli such as nutrients, chemoattractants, cytokines, hormones, growth factors, morphogens, and environmental stressors (Table 1) change in diverse patterns that include variations in the

intensity, duration, time between sequential stimulations, rate of change, non-linearity, and combinations of different dynamics (Figure 1; Table 2). As a result, cell responses can change as a function of different gradual and acute environments. Despite these facts, most ongoing biological research measures responses to a limited number of instantaneously changing environments (dose-response curve) in cell populations (Figure 1A) (Lim et al., 2014; Alberts et al., 2015). These studies often use normal or mutant cells to understand how genetic differences or disease impact signaling response and cell phenotype. In Figure 2, we conceptually illustrate the phenotype relationship between stimulus molecules (red axis), genetic backgrounds (blue axis), and dynamic change of the stimulus molecule (green axis). The stimulus molecules axis represents any molecule or molecule combinations that can activate or repress a process in a cell, causing a phenotypic change. This axis includes all drugs and their combination that can impact the cell. This number is infinite, given the various molecules and drugs. The genetic background axis represents any genetic change affecting cell behavior and phenotype. It is also easy to assume that unique genetic constellations are infinite. The third axis presents the different dynamic changes of the stimulus molecule with which any given stimulus molecule can change over time for any given genetic background (Figure 1B–F). However, most biomedical laboratory research uses a finite set of acute changes in the stimulus molecule concentrations (Figure 1A). A typical example of such a study is the classical dose-response experiment that may use a dozen different concentrations (Figure 2, black circle).

In contrast, cells of any organism or in any natural environment experience a wide variety of gradual changes in external stimuli. Current treatments and therapies are based on observed phenotypes (purple plane) and current disease models (grey star) in such acute treatments, potentially missing or misinterpreting the response of a cell to the stimulus under physiological conditions. For example, if one uses a dozen concentrations from the previously mentioned dose-response experiment and alters the concentration acutely every 1 min for 30 min, then there are $12^{30} = 2.3 \times 10^{32}$ unique combinations possible. This simple example demonstrates the possible infinite space of modulating the environment of cells in a non-acute manner. This new dimension of dynamic changes of the stimulus molecule may dramatically expand our phenotypic space currently not explored in the laboratory (white star). Including this critical dimension will allow us to observe physiologically relevant phenotypes in different dynamic phenotypes (yellow plane) and under different genetic backgrounds (cyan plane). By designing experiments that consider this new dimension of dynamic changes of the stimulus molecule, we expect to better characterize the accurate and relevant biomedical phenotype (white star) compared to current disease models (grey star) that do not fully consider this new dynamic dimension. As an example of the latest insights gained from dynamic temporal environments, we will focus on the newly discovered concept of a rate threshold. Similar to a concentration threshold, where a concentration above a certain value activates signaling, a rate threshold is a value in the rate of change in the environment that needs to be crossed to activate

TABLE 1 Environment type that changes over time.

Environment type	Citations
Nutrients	Block et al. (1983), Segall et al. (1986), Tu et al. (2008), Shimizu et al. (2010)
Chemoattractants	Wang et al. (2012), Chang and Levchenko (2013), Sgro et al. (2015)
Cytokines	Luecke et al. (2021), Meizlish et al. (2021)
Hormones	Bratusch-Marrain et al. (1986), Polonsky et al. (1988), Fernandez and Torres-Alemán (2012), Kubota et al. (2012), Kubota et al. (2018), Noguchi et al. (2013), Sano et al. (2016)
Growth factors	Sasagawa et al. (2005), Fujita et al. (2010), Ji et al. (2010), Avraham and Yarden (2011), Fernandez and Torres-Alemán (2012), Sorre et al. (2014)
Morphogens	Wang et al. (2012), Sorre et al. (2014), Dubrulle et al. (2015), Sagner and Briscoe (2017), Tewary et al. (2017); Hill (2018), Heemskerk et al. (2019), Li and Elowitz (2019), Mateus et al. (2020), Hashmi et al. (2022)
Environmental stressors	Neuhof and Beck (2005), Muzzey et al. (2009), Pelet et al. (2011), Young et al. (2013), Carlström et al. (2015), Nguyen-Huu et al. (2015), Goulev et al. (2017), Granados et al. (2017), Firsov and Bonny (2018), Thiemicke et al. (2019), Jashnsaz et al. (2020), Jashnsaz et al. (2021), Johnson et al. (2021), Thiemicke and Neuert (2021)

TABLE 2 Different dynamics of the same environment.

Environment dynamics	Citation
Intensity	Hersen et al. (2008), Mettetal et al. (2008), Macia et al. (2009), Muzzey et al. (2009), Pelet et al. (2011), Neuert et al. (2013), Granados et al. (2017), Jashnsaz et al. (2020)
Rate of change	Block et al. (1983), Sasagawa et al. (2005), Muzzey et al. (2009), Fujita et al. (2010), Shimizu et al. (2010), Pelet et al. (2011), Kubota et al. (2012), Kubota et al. (2018), Wang et al. (2012), Young et al. (2013), Sorre et al. (2014), Sgro et al. (2015), Heemskerk et al. (2019), Thiemicke et al. (2019), Johnson et al. (2021), Thiemicke and Neuert (2021)
Duration	Hersen et al. (2008), Mettetal et al. (2008), Mitchell et al. (2015), Gunne-Braden et al. (2020)
The time between sequential stimulations	Hersen et al. (2008), Mettetal et al. (2008), Mitchell et al. (2015), Rahi et al. (2017), Jashnsaz et al. (2020), Johnson et al. (2021)
Combinations of environment dynamics	Bandara et al. (2009), Wang et al. (2012), Sgro et al. (2015), Jashnsaz et al. (2020), Jashnsaz et al. (2021), Johnson et al. (2021)

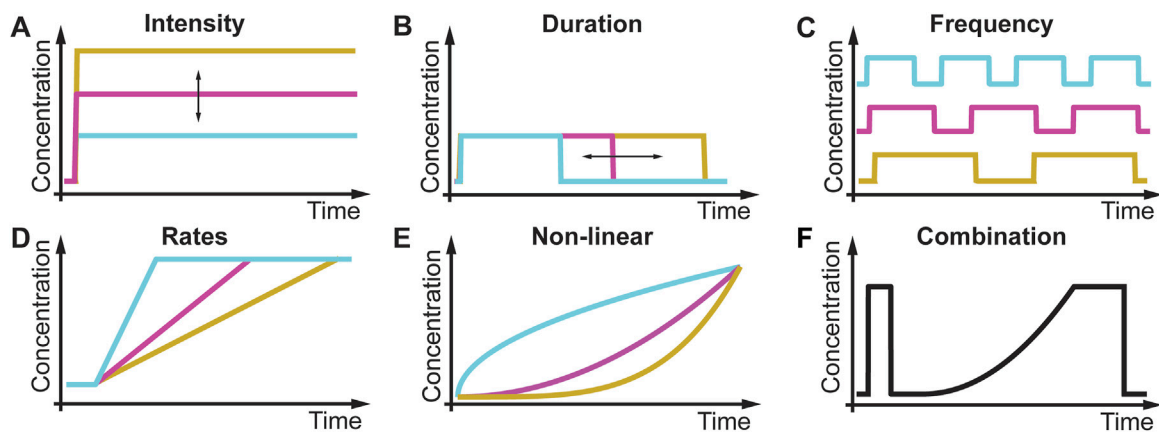


FIGURE 1 Different environmental dynamics in biology and laboratory research. (A) In a dose-response experiment, the intensity of a stimulus changes acutely. (B) Duration of stimulus changes. (C) Frequency of stimulus changes. (D) Rate of the stimulus changes. (E) Non-linearity of the stimulus changes. (F) Each of these stimulus patterns can be combined to generate infinite numbers of environmental dynamics.

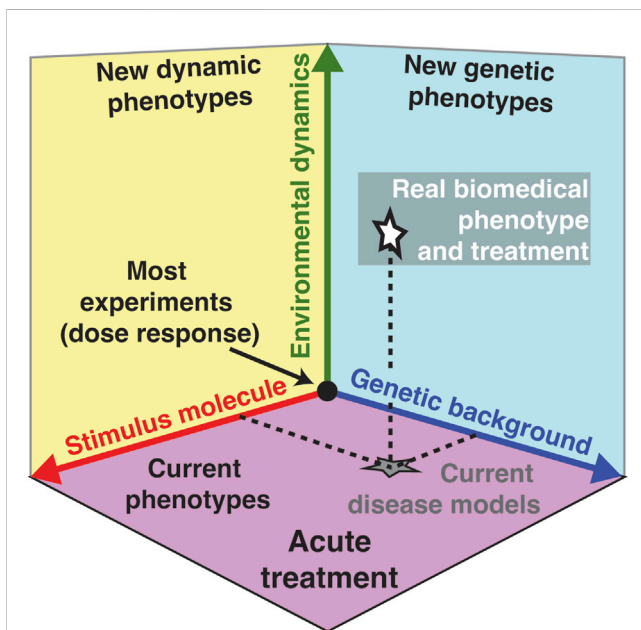


FIGURE 2 Environmental dynamic of the stimulus molecule as a new dimension in biomedical research. Phenotype relationship between stimulus molecules or drugs (red axis), genetic background (blue axis), and environmental dynamics (green axis). Each combination of these three axis can define a unique phenotype. Because current environmental dynamics often only consider dose-response experiments using acute environmental changes, the green axis effectively projects onto the purple plane that describes most observed present phenotypes, disease models, and treatment regimes (gray star). Environmental dynamics add variety to the types of environmental changes investigated (green arrow) and increase the dimensionality of biological knowledge to new dynamic phenotypes (yellow plane) and new genetic phenotypes (cyan plane), thereby providing a more accurate picture of physiologically relevant biology and biomedicine (white star).

signaling. We argue that a rate threshold is a novel and phenotypically important mechanism in cell signaling that is relevant in gradual and non-acute changing environments. In this review, we will focus on pathways that respond to gradual environmental changes and describe different examples from the literature to illustrate the importance of non-acute and gradually changing environments from bacteria to humans. We will start with a yeast Mitogen-Activated Protein Kinase (MAPK) pathways rate sensitivity and rate threshold as a paradigm for all the remaining pathways.

2 Concentration and rate thresholds regulate yeast stress response

The high osmolarity glycerol (HOG) MAPK pathway in the budding yeast *Saccharomyces cerevisiae* (Figure 3A) is an ideal model system (Brewster et al., 1993; Saito and Posas, 2012; Brewster and Gustin, 2014) for addressing the question how do rate sensitivity and rate thresholds impact cell signaling and phenotype (Thiemicke et al., 2019; Jashnsaz et al., 2020; Johnson et al., 2021). At the molecular level, pioneering studies found that one signaling branch is activated through the Synthetic Lethal of N-end rule (Sln1) osmosensing histidine protein kinase leading to activation of the MAPKKK’s Suppressor of Sensor Kinase (Ssk2) and its paralog Ssk22 and converging on the MAPKK Polymyxin B Sensitivity (Pbs2) kinase through several intermediate proteins. Another signaling branch is activated through the Synthetic, High Osmolarity-sensitive (Sho1) signaling protein osmosensor that activates the STerile Signal transducing MEK kinase (STE11) converging on Pbs2 (Maeda et al., 1994; Posas et al., 1996; Posas and Saito, 1997; Macia et al., 2009; Saito and Posas, 2012). Activated Pbs2 then dually phosphorylates the evolutionarily conserved MAPK Hog1 on threonine residue 174 (T174) and

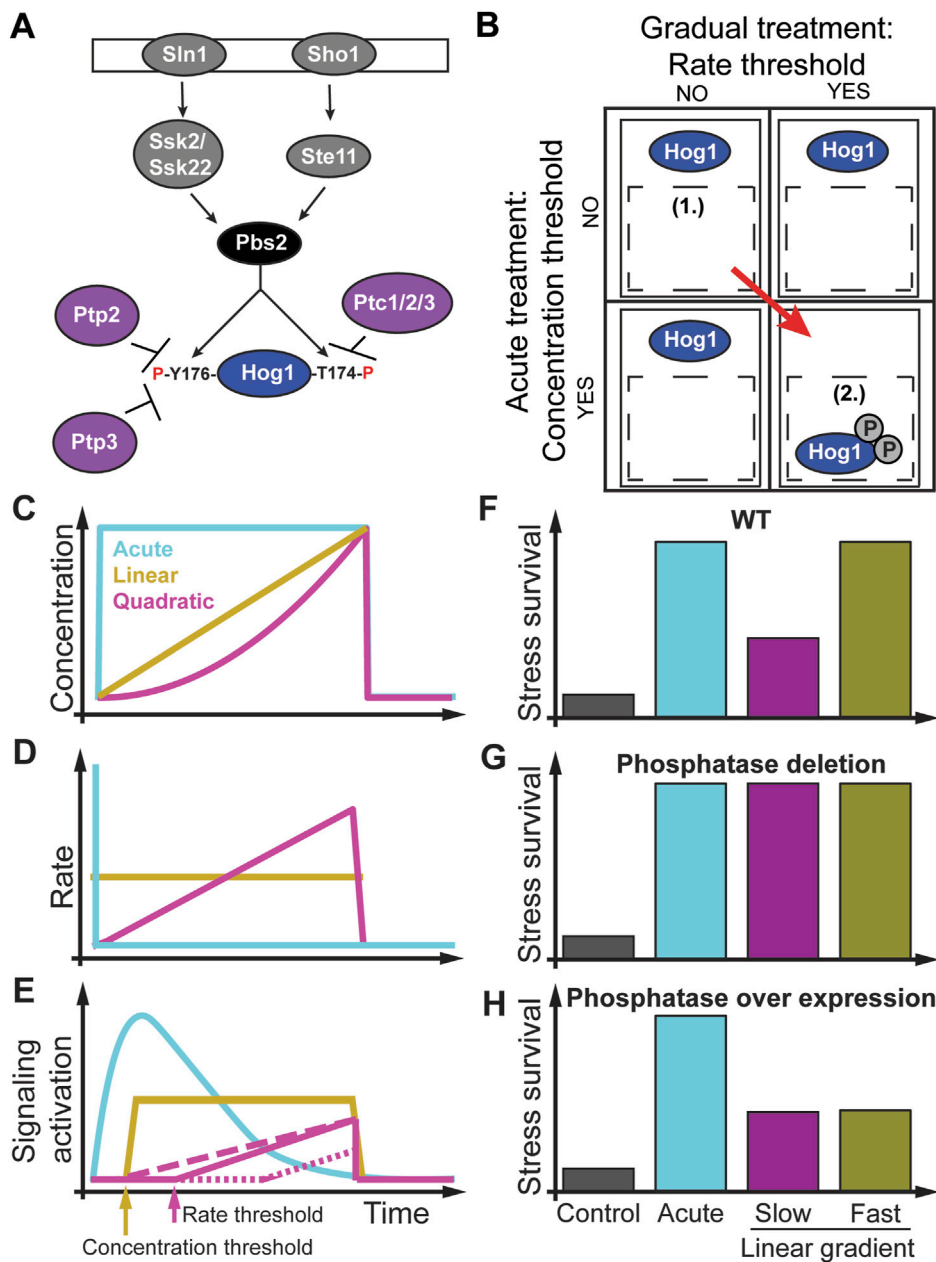


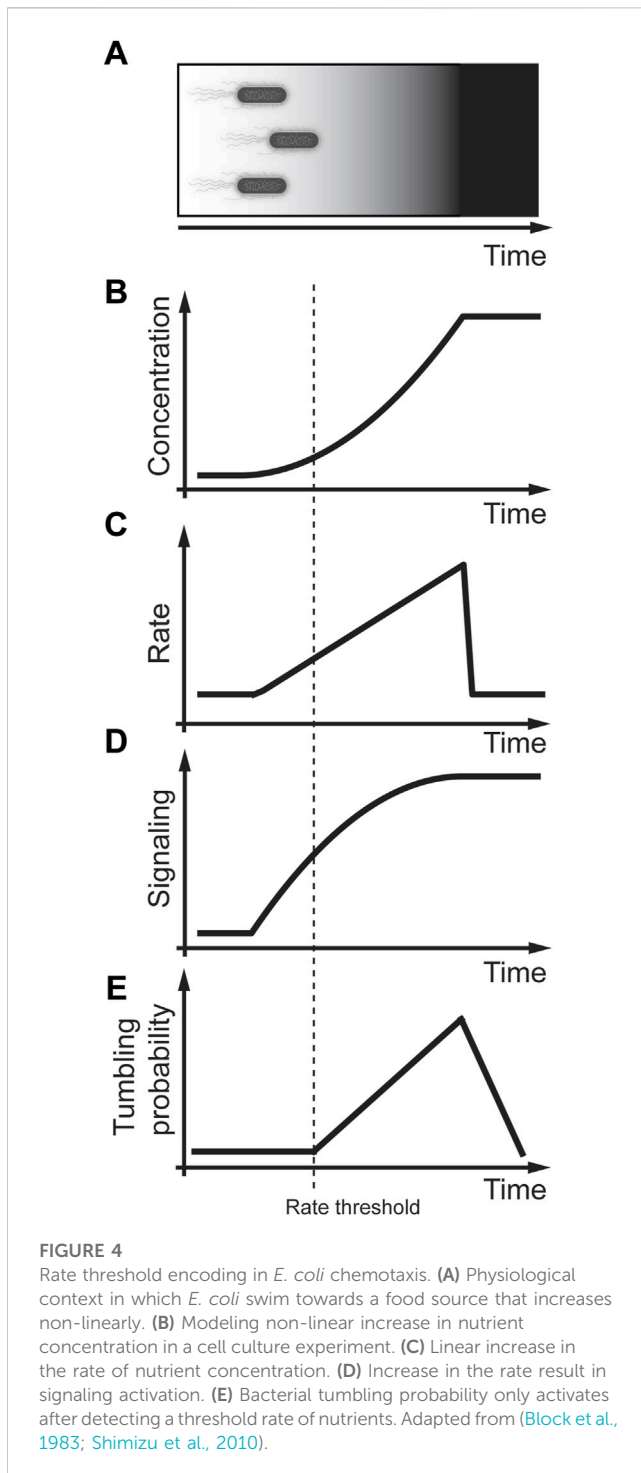
FIGURE 3 Rate threshold encoding in the yeast HOG pathway. **(A)** Components of the High Osmolarity Glycerol MAPK pathway. **(B)** Non-acute treatments such as linear and quadratic osmolyte gradients discovered a rate threshold with a concentration threshold regulating Hog1 MAPK through an AND logic. **(C)** Different osmolyte concentration profiles as a function of time. **(D)** Rate changes for these concentration changes. **(E)** Hog1 signaling activation depends on the cell environmental dynamics and pathway mutants. For a linear concentration increase with a rate above the rate threshold (sand line), signal activation increases after a concentration threshold is met (sand arrow). For a quadratic concentration increase (magenta line) resulting in a linear increase in the rate, the concentration threshold is met earlier than the rate threshold (magenta arrow), and Hog1 gets activated (magenta solid line). Phosphatase deletion removed the rate threshold (magenta dashed line). Overexpression of the phosphatase increases the rate threshold (magenta dotted line). **(F)** A stress-resistant assay shows increase survival of acute (cyan bar) and fast (yellow bar) but not slow (magenta bar) stressed cells. **(G)** Deletion of phosphatase makes cells resistant to rate changes. **(H)** Overexpression of phosphatase makes cells hyper-sensitive to rate changes but not to acute changes. Adapted from (Johnson et al., 2021).

tyrosine residue 176 (Y176) (Saito and Posas, 2012). This dual phosphorylation is required for Hog1 nuclear import (Figures 3A, B) (Ferrigno et al., 1998; Westfall and Thorner, 2006). Once in the nucleus, the activated Hog1 regulates the expression of several hundred stress response genes (Gasch et al., 2000; Rep et al., 2000;

Capaldi et al., 2008; Pelet et al., 2011; Neuert et al., 2013; Nadal-Ribelles et al., 2014). Hog1 can be inactivated by the phosphotyrosine-specific phosphatases Ptp2 and Ptp3 and the type 2C protein phosphatases (PP2C) Ptc1, Ptc2, and Ptc3 (Jacoby et al., 1997; Wurgler-Murphy et al., 1997; Mattison and

Ota, 2000; Warmka et al., 2001; Young et al., 2002; Mapes and Ota, 2004; Saito and Posas, 2012). Among these phosphatases, only Ptc1 uses an adaptor protein (the Nap binding protein Nbp2) to transiently interact with Pbs2 (Mapes and Ota, 2004; Stanger et al., 2012). The multiple and presumably redundant MAPK phosphatases dephosphorylate and inactivate Hog1, which, along with the termination of upstream signaling after adaptation, results in its return to the cytosol. This knowledge of the Hog1 pathway was established through acute osmotic stress concentration increases that induce Hog1 phosphorylation, activation, and translocation to the nucleus (Figures 3A, B) (Brewster et al., 1993; Ferrigno et al., 1998; Reiser et al., 1999; Hersen et al., 2008; Macia et al., 2009; Muzzey et al., 2009; Pelet et al., 2011; Saito and Posas, 2012; English et al., 2015; Mitchell et al., 2015; Granados et al., 2017). Activated Hog1 controls the regulation of cellular osmoadaptation and survival (Saito and Posas, 2012; Mitchell et al., 2015; Johnson et al., 2021). Because of this behavior of Hog1 nuclear enrichment, single-cell time-lapse microscopy and analysis have proven an excellent and sensitive way to monitor signaling responses to dynamic stimulation patterns in real-time (Figure 3) (Hersen et al., 2008; Mettetal et al., 2008; Muzzey et al., 2009; Patterson et al., 2010; Munsky et al., 2012; Mitchell et al., 2015; Granados et al., 2017; Thiemicke et al., 2019; Jashnsaz et al., 2021; Johnson et al., 2021). This single-cell analysis of Hog1 nuclear localization response to instant osmotic stress resulted in the discovery of perfect adaptation in this pathway (Figures 3C–E) (Hersen et al., 2008; Mettetal et al., 2008; Muzzey et al., 2009). Perfect adaptation means that the pre and post-stimulus signal is identical. Because of adaptation, the Hog1 pathway is sensitive to the concentration and rate of external stimulus. Pioneering studies then used increasing linear gradients of osmolytes to test the adaptation model (Figures 3C–E) (Muzzey et al., 2009). The proposed network motif to achieve perfect adaptation in this pathway is the integral feedback loop (Stelling et al., 2004) by which the cell integrates up internal glycerol and computes the pressure difference between outside and inside the cell (Mettetal et al., 2008; Muzzey et al., 2009). Almost a decade later, several osmolyte rates were used to dissect the contribution of the different upstream Hog1 signaling branches showing how each branch has a slightly different rate dependence in regulating Hog1 nuclear enrichment (Granados et al., 2017). However, neither of these studies considered how these different osmolyte gradients regulate growth or survival phenotypes. Another study using square waves of osmolytes of different duration showed that fast and slow fluctuating osmolyte environments do not alter yeast doubling time. However, fluctuations with intermediate durations resulted in a fourfold reduction in yeast growth rate, showing that environmental fluctuations have phenotypic consequences (Mitchell et al., 2015). Several labs developed novel cell culture assays to expose cells to non-acute environmental changes, followed by quantitative experiments to investigate molecular mechanisms in non-acute environmental conditions (Figures 3C, D) (Block et al., 1983; Muzzey et al., 2009; Fujita et al., 2010; Shimizu et al., 2010; Pelet et al., 2011; Kubota et al., 2012; 2018; Wang et al., 2012; Noguchi et al., 2013; Sgro et al., 2015; Mokashi et al., 2019; Thiemicke et al., 2019; Krause et al., 2021). The novel experimental setup developed by Thiemicke et al. recently investigated how Hog1 signaling and cell viability are impacted by different rates of osmolyte gradients

(Figures 3C–H) (Johnson et al., 2021). In Figure 3C, the authors applied acute (cyan line), linear (sand line), and quadratic (magenta line) concentration changes with the same final concentration and duration to yeast cells. These concentration changes result in no rate changes for acute stresses (cyan line), a constant rate change for a linear concentration increase (sand line), or a linear rate increase for a quadratic concentration increase (magenta line) (Figure 3D). As a result of these concentration profiles (Figure 3E), Hog1 signal activation adapted perfectly upon acute concentration changes (cyan line). Upon a linear stress increase, Hog1 activates with a delay after reaching a concentration threshold (sand arrow) followed by constant signal amplitude (sand line). Interestingly, exposing yeast cells to a quadratic stress increase resulted in a longer delay in Hog1 activation due to a threshold in the rate (magenta line and arrow). Only after a threshold rate was reached did the Hog1 signaling increase linearly. In detailed experiments, they showed that Hog1 nuclear localization depends on an osmolyte concentration and a rate threshold. Additional experiments showed that the Hog1 pathway uses an AND logic to integrate the previously determined concentration threshold (Macia et al., 2009) and the rate threshold. Both thresholds are required to activate Hog1 nuclear localization. Figure 3B shows how different stress treatment dynamics can probe one or the other threshold. The authors then used different linear osmolyte gradients to the same final and total osmolyte concentration below and above the threshold rate, followed by a second severe stress. Using a colony formation assay, they found that cells treated with a pulse or a linear osmolyte gradient above the threshold rate survive ten times better than untreated cells (Figure 3F). However, cells treated with a linear increasing osmolyte gradient below the rate threshold survived only five times better than untreated cells, demonstrating that the rate of the gradient determines cell survival. In these experiments, the dose defined as the integrated NaCl exposure is identical between the different experiments, but the viability phenotype is different. They then investigated the molecular basis of this rate threshold by performing a targeted genetic knockout screen and identified the phosphatase Ptp2 but not the seemingly redundant Ptp3 as a rate threshold regulator leading to earlier activation of Hog1 nuclear localization only dependent on the threshold concentration (Figure 3E, dashed magenta line). The knockout of Ptp2 was then rescued by varying the expression level of Ptp2, showing that the threshold rate is proportional to the expression level of Ptp2 (dotted magenta line). Subsequent colony formation experiments showed that the deletion of Ptp2 made cells resistant to osmolyte gradients (Figure 3G). In contrast, overexpression of Ptp2 made cells hypersensitive to osmolyte gradients but not to acute osmolyte changes (Figure 3H). These results demonstrate that gradient environmental changes regulate cellular phenotypes. Yeast cells use a novel rate threshold mechanism to differentiate between different rates of stimulus increase. Moreover, “redundant phosphatases” have specific non-redundant functions only detectable in non-acute environmental conditions. We speculate that a possible network motives that could give rise to such a rate threshold in an adapting system is a combination of a Hill function with a negative feedback loop or with an incoherent feed forward loop (Milo et al., 2002; Ma et al., 2009; Rahi et al., 2017). In the context of signal transduction, a Hill function describes the



relationship between the concentration of a ligand and the non-linear activation of a downstream signaling protein. A negative feedback loop is the regulation of an upstream signaling protein through a downstream signaling protein. An incoherent feed forward loop has the property to activate both a target signaling protein and an inhibitor of that proteins, which then inhibits the target signaling protein. This study hypothesized that the novel rate threshold mechanism in cell signaling might be prevalent in other pathways and organisms, which is the focus of this review

article. We next describe how rate sensitivity and thresholds are prevalent in bacterial chemotaxis.

3 *E. coli* chemotaxis nutrient sensing

Chemotaxis is a process that allows bacteria to sense nutrients in their surrounding by randomly sampling their environments and then measuring the nutrient concentration over time (Figure 4A) (Adler and Alon, 2018; Tu and Rappel, 2018). Although chemotaxis in bacteria is molecularly well understood (Waite et al., 2018; Karmakar, 2021), the physiological relevance leaves many open questions (Colin et al., 2021; Keegstra et al., 2022). The core signal transduction pathway responsive to chemotaxis in *E. coli* is reviewed in detail by (Waite et al., 2018; Karmakar, 2021). Here we briefly summarize the chemotaxis pathway that consists of a membrane-associated receptor kinase complex A that can sense an external ligand concentration [L]. Activation of complex A regulates the autophosphorylation activity resulting in a phosphate transfer to the response regulator CheY leading to phosphorylated CheY (CheY-P). CheY-P then interacts with the flagellar motor M to control swimming. The activity of CheY is determined by the phosphorylation of CheY through the histidine kinase ChrA and dephosphorylation through the phosphatase CheZ. The receptor kinase complex A is regulated through feedback consisting of the methyltransferase CheR and the methylesterase CheB that modified the number of methylated glutamyl residues. Early studies of quantifying *E. coli* tumbling frequency discovered that acute exposure to nutrients resulted in an instant response that perfectly adapted to the initial conditions within a few seconds (Block et al., 1982). This response was explained through a model by an integral feedback loop from the receptor kinase complex A activating the phosphorylated methylesterase/deamidase CheB-P. CheB, CheB-P, and methyltransferase CheR then provide feedback to regulate the receptor methylation of the receptor kinase complex A (Shimizu et al., 2010). A vital property of an adaptive system is that it is sensitive to the concentration and the rate of change of the external ligand.

Further understanding of this adaptive behavior was acquired through carefully controlled *in vitro* experiments using exponentially increasing and decreasing gradient profiles of external ligands (Figures 4B, C) (Block et al., 1983; Segall et al., 1986; Shimizu et al., 2010). Shimizu et al. (2010) performed elegant fluorescence resonance energy transfer (FRET) experiments between CheY, and CheZ, genetically tagged with a yellow fluorescent protein (YFP) and cyan fluorescent protein (CFP), respectively. The measured FRET signal is a live cell readout that approximates CheY-P, the phosphorylated form of CheY. These studies showed that even small increases in the rate of the external ligand lead to CheY signaling (Figure 4D) (Shimizu et al., 2010). In contrast, carefully controlled experiments measuring the rotational probability of the flagellum by Block et al. (1983) showed that there is a potential rate threshold that the ligand needs to overcome to activate the flagellum motor (Figure 4E). This rate threshold was explained as a time delay required to measure the rate changes (Block et al., 1983). An alternative explanation is that the amount of CheY-P or rate change of CheY-P might need to overcome a threshold similar to the rate threshold in MAPK signaling in yeast cells (Johnson et al., 2021). To address this hypothesis, future studies need to expose *E. coli* to different concentration gradients and measure CheY-P as a signaling readout and the *E. coli* tumbling frequency as an activity readout. Ideally, these experiments

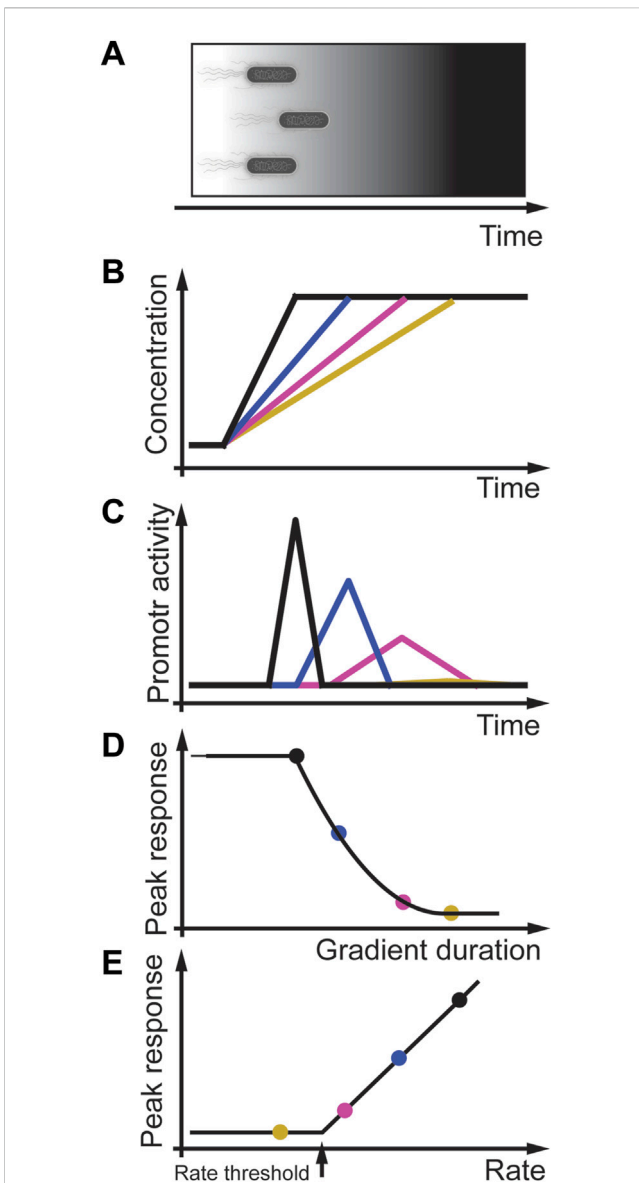


FIGURE 5
Rate threshold encoding in *B. subtilis* stress response. (A) Physiological context in which *B. subtilis* experience an increasing stress gradient. (B) *In-vitro* modeling of different linear gradients of osmotic stress. (C) Gene expression promoter activity is transient and dependent on the stress rate. (D) Peak response (colored solid circles) decreases with gradient duration and decreasing rate. (E) Peak response as a function of the rate indicate that *B. subtilis* stress response may encode a rate threshold. Adapted from (Young et al., 2013).

could then be repeated in other mutant strains of the chemotaxis pathway to identify potential proteins that regulate the rate threshold.

4 Bacterial *B. subtilis* stress response

Another example of rate sensitivity in prokaryotes is the general stress response in the bacterium *B. subtilis* (Figure 5A) (Hecker et al., 2007). In this bacterium, different stressors activate the stressosome that regulates the availability of the serine/threonine-protein kinase RsbT.

RsbT phosphorylates the phosphoserine phosphatase RsbU, which then dephosphorylates RsbV, an anti-sigma-B factor antagonist. The binding of RsbV to the serine-protein kinase RsbW results in the release of sigma factor σ^B that activates target promoters, including its operon, the phosphatase RsbX, and induces other genes of the environmental stress response. Expression of RsbX negatively regulates and feedbacks to RsbT. This feedback is essential for the adaptive behavior of *B. subtilis* to instant environmental stress (Young et al., 2013). In carefully controlled experiments, Young et al. (2013) showed that the amplitude of a transcriptional single-cell reporter is proportional to the intensity of the acute and instant stressors NaCl, ethanol, and butanol (Figures 5B, C) consistent with population studies (Boylan et al., 1993). As expected from an adaptive system, when NaCl or ethanol stress increases at different rates, the amplitude of the σ^B promoter response changes proportional to the gradient rate (Figure 5D) (Young et al., 2013). However, at very shallow rates to a high-stress concentration of NaCl or ethanol, the promoter response was similar to non-stressed cells, indicating that stress response in *B. subtilis* may also be regulated by a rate threshold (Figure 5E). Further studies must be performed using different linear and quadratic stress gradients in normal and mutated bacteria to investigate this potential rate threshold mechanism.

5 Rate sensitivity in amoebae response

Besides single-cell organisms, rate sensitivity, and rate thresholds were also observed in cells of multicellular organisms. This section will focus on the chemoattractant cyclic adenosine monophosphate (cAMP) sensitivity of single *Dictyostelium* cells (Figure 6A) (Artemenko et al., 2014; Nichols et al., 2015). These single cells can use cell-to-cell communication through cAMP to coordinate collective cell behavior, the basis for the slug and fruit body formation process. Figure 6A illustrate a situation in which a cell secretes cAMP (green cell), and cells in the neighborhood (black, blue, magenta, yellow cells) sense different temporal gradient in cAMP dependent on their distance to the secreting cell (grey gradient). The signaling process involves cAMP binding to cAMP-specific heterotrimeric guanosine triphosphate-binding protein (G protein)-coupled receptors (GPCRs). These GPCRs then transiently activate phosphoinositide 3-kinase (PI3K), which then adapts to persistent and constant cAMP concentrations. A fundamental question is how individual *Dictyostelium* cells sense cAMP changes in their environment over time, as in the process from a single cell to a multicellular organism. To address this question in a controlled environment, Wang et al. (2012) and Sgro et al. (2015) designed experiments in which they changed the dynamics of the cAMP concentrations over time (Figures 6B, D, F). Wang et al. (2012) developed a sophisticated microfluidic chip to generate acute and slowly changing cAMP concentrations at different rates (Figure 6B). They used a phosphatidylinositol 3,4,5-trisphosphate (PIP3)-specific biosensor to monitor its kinetics to the plasma membrane as a live cell readout of cAMP signaling (Figure 6C). Similar to previous studies, they observed rapid transient and adapting biosensor translocation. With this experimental setup, they experimentally and computationally studied the cAMP signaling response to better understand the underlying effective signaling network

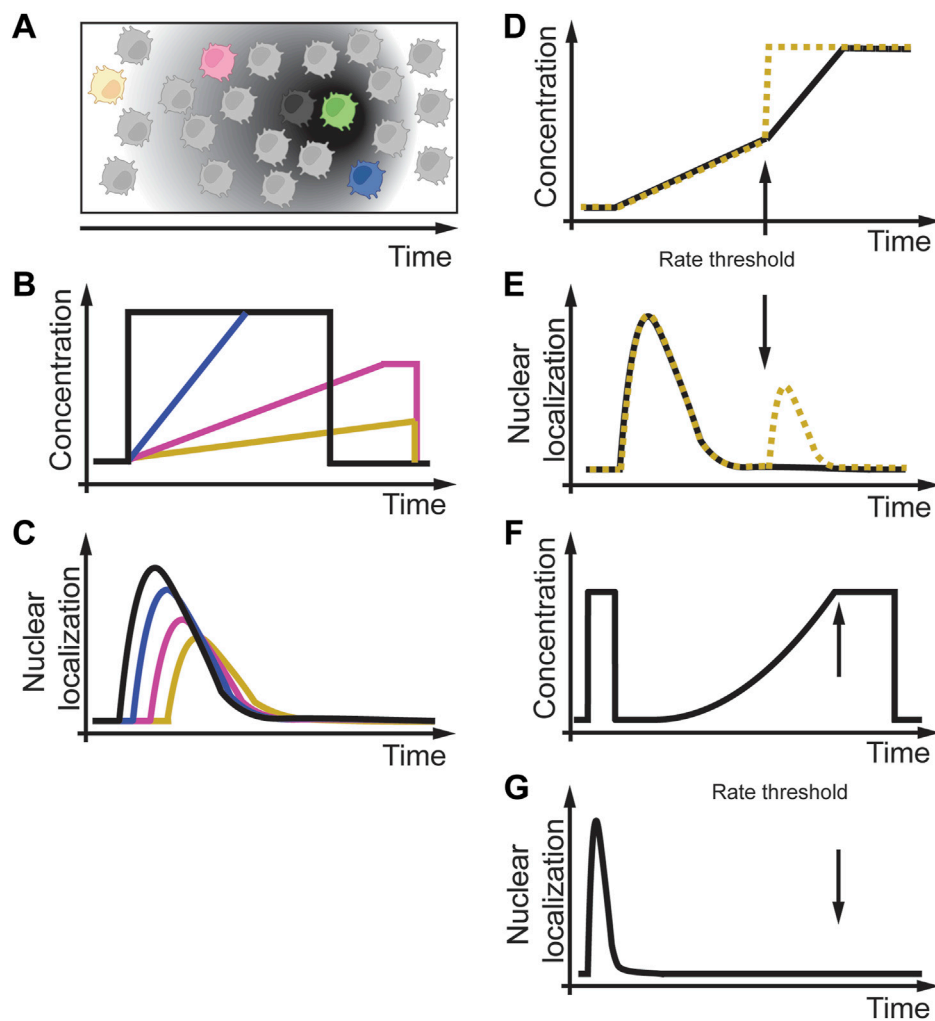


FIGURE 6

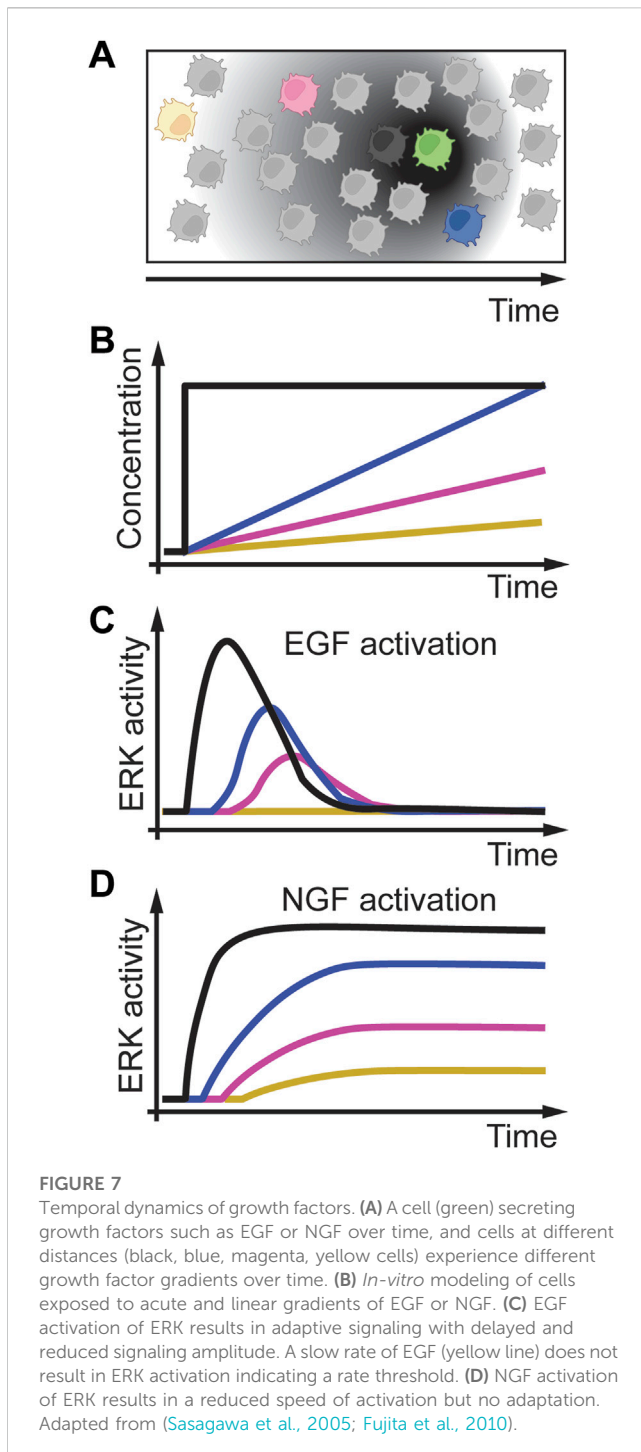
Rate sensitivity and rate threshold in amoeba *Dictyostelium discoideum*. (A) A *D. discoideum* cell (green) is secreting cAMP over time, and cells at different distances (black, blue, magenta, yellow cells) experience different acute and linear cAMP gradients over time. (B) *In-vitro* modeling of different acute and linear cAMP gradients over time. (C) Different temporal cAMP gradients result in delayed and reduced activity of cAMP signaling. (D) Exposure of *Dictyostelium* cells to two different cAMP profiles with the same initial rate and a subsequent faster rate (black solid line) or an acute increase (yellow dashed line). (E) *Dictyostelium* cells respond to a slow first treatment rate but only to an acute second treatment (yellow dashed line) and not to a slow second treatment (black solid line), indicating a rate threshold. (F, G) Non-linear gradients below a possible threshold rate do not activate cAMP signaling. Adapted from (Wang et al., 2012; Sgro et al., 2015).

structure. As part of their studies, they used linearly increasing cAMP gradients of different rates. They experimentally found that decreasing the cAMP rate led to a delay and reduced amplitude in biosensor readout (Figure 6C). Interestingly, when they used two different subsequent rates (Figure 6D), of which the first rate was fast. Still, the second rate was slow (Figure 6D, black line), the cell did not respond to the second slow rate cAMP stimulus (Figure 6E, black line), whereas if the second rate was fast (Figure 6D, yellow dashed line), cells responded (Figure 6E, yellow dashed line). Similarly, in *Dictyostelium* cells, Sgro et al. (2015) showed that signaling due to an exponential cAMP increase starts to oscillate above a certain rate threshold (Figures 6F, G). These results indicate that cAMP signaling in *Dictyostelium* cells is rate sensitive and

contains a rate threshold. However, the mechanism and protein(s) decoding these rate thresholds within the same or different cells is elusive and requires further studies.

6 Temporal dynamics of growth factors in mammalian cells

Growth factors are molecules that stimulate cell proliferation and growth. These molecules change over time in various tissues and organisms (Figure 7A) (Fernandez and Torres-Alemán, 2012; Li and Elowitz, 2019; Koseska and Bastiaens, 2020). A long-studied system of growth factor signaling is the dynamic activation of the extracellular-signal-regulated kinase (ERK) signaling network



through the epidermal growth factor (EGF) and nerve growth factor (NGF) (Avraham and Yarden, 2011). Extracellular EGF binds to the EGF receptor (EGFR), which then, through several proteins, activates the Rat sarcoma virus (RAS) protein. RAS then transiently activates ERK. When extracellular NGF is present, it can bind to the Tropomyosin receptor kinase A (TrkA). TrkA then activates Ras-related protein 1 (Rap1), resulting in sustained ERK activation. Traditional studies used PC12 cells, a rat pheochromocytoma cell line, to model this pathway response to growth factors. They applied acute concentration changes of EGF

(Figure 7B, black line) that resulted in adaptive ERK signaling (Figure 7C, black line). In contrast, acute increasing concentrations of NGF resulted in sustained ERK signaling (Figure 7D, black line). To better understand this pathway and to validate computational predictions, Sasagawa et al. (2005) exposed PC12 cells to linearly increasing concentrations of EGF and NGF at different rates (Figure 7B, colored lines). As expected from an adaptive system, slower rates of EGF resulted in adaptive but reduced ERK signaling intensity (Figure 7C, colored lines), whereas slow rates of NGF resulted in sustained but slower ERK activation (Figure 7D, colored lines). Interestingly, slow-increasing EGF concentration resulted in no ERK activation, whereas acute EGF increases resulted in robust ERK activation. These results on linear EGF gradients activating ERK were confirmed in a subsequent study from the same group, indicating that ERK signaling through EGF might also be rate threshold dependent (Fujita et al., 2010). In this study, Fujita et al. showed that cell proliferation markers pAKT (phosphorylated Protein kinase B) and Ribosomal protein S6 show rate-sensitive signaling. These results indicate that pAKT and S6 might also have a rate threshold.

In an independent study, Ji et al. (2010) exposed cultured rat hippocampal neurons to acute and gradual increases in the brain-derived neurotrophic factor (BDNF). BDNF is a neuropeptide important for synaptic development and plasticity (Park and Poo, 2012; Wang et al., 2022). BDNF binds and activates the TrkB receptor tyrosine kinase, which activates downstream MAPK, phosphatidylinositol-3 kinase (PI3K), and Phospholipase C, gamma 1 (PLC- γ) pathways. One central question by Ji et al. is how different dynamics of BDNF activate signaling and regulate phenotype. They found that acute administration of BDNF to primary neurons resulted in adaptive phosphorylation of TrkB and ERK. In contrast, a logarithmic increase in BDNF resulted in a gradual and sustained activation of the same proteins. A significant conclusion from this study was that BDNF delivery rate might be the primary regulatory mechanism rather than the absolute BDNF concentration. As a mechanism, they showed that the Ras-MAPK complex is transiently activated in acute and gradual conditions. In contrast, the Rap1-MAPK complex is transiently activated in acute situations and sustainably activated in gradual conditions. Ji et al. also showed that PLC- γ 1 and Glycogen synthase kinase-3 beta (GSK-3 β) behave similarly to ERK, suggesting that the rate sensitivity is encoded upstream of ERK, PLC- γ 1, and GSK-3 β signaling. Downstream, differences in ERK signaling were mirrored by the phosphorylation dynamics of the cAMP response element-binding protein (CREB) transcription factor. The different dynamics of CREB phosphorylation and activation are essential for long-lasting synaptic effects of BDNF and result in differential gene expression of immediate early genes. These changes then also affected dendritic growth and the morphological specializations of dendrites of young hippocampal neurons where acute BDNF treatment promotes neurite growth, whereas gradual BDNF treatment regulates neurite branching. Ji et al. then quantified dendritic spine growth to demonstrate the importance of acute and gradual BDNF administration in mature neurons. They showed that acute treatment with BDNF resulted in more spines with larger heads, whereas gradual BDNF regulates the length of spines and the outgrowth of filopodia-like protrusions. They also showed in hippocampal slices as an *in vivo* system that acute BDNF

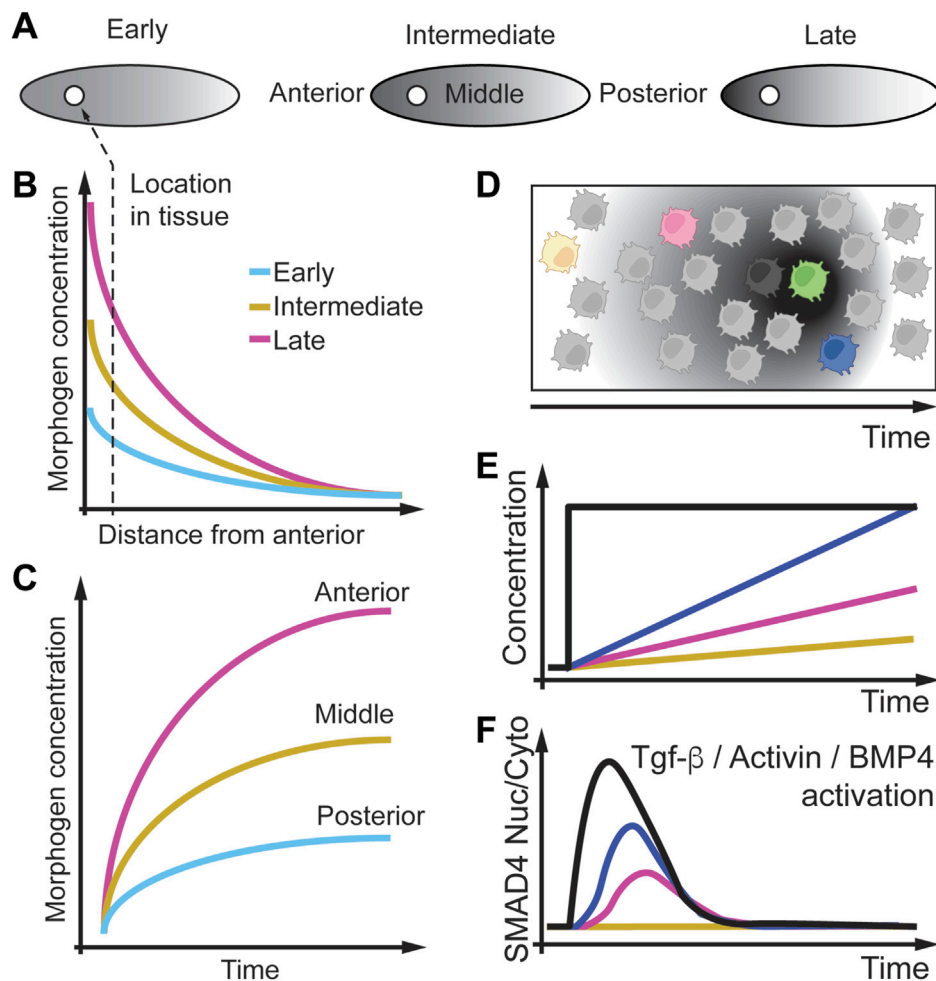


FIGURE 8

Morphogen gradients change as a function of space and time. (A) Morphogen gradients form between the anterior and posterior of a fly embryo and change over time from early to late in development. (B) The morphogen gradient decreases along the anterior and posterior axis, starting at a lower concentration at early time points. (C) The same data is plotted as a function of time, where nuclei at different positions experience different gradients. (D) Modeling morphogen gradients *in vitro*. (E) In cell culture different cells can experience different morphogen gradients over time. (F) Ratio of nuclear to cytoplasmic SMAD4 as a real-time readout is sensitive to the rate of Tgf- β , Actevin, or BMP administration. Slow rates (yellow line) of Tgf- β , Actevin, or BMP administration does not result in SMAD4 nuclear localization, indicating a rate threshold. Adapted from (Sorre et al., 2014; Heemskerk et al., 2019).

enhances basal synaptic transmission and that gradual BDNF exposure facilitated long-term potentiation (LTP). These results show that the dynamics of BDNF differentially regulate cell signaling and phenotypes and indicate that BDNF signaling is rate sensitive, and this pathway may encode a rate threshold. Further studies are required to establish this rate sensitivity, the rate threshold, and the proteins regulating these processes.

7 Spatio-temporal dynamics of morphogens

Another important class of signaling molecules that change in space and time are morphogens which are non-uniformly distributed molecules that regulate cell fates during

development (Dessaud et al., 2007; Kutejova et al., 2009; Rushlow and Shvartsman, 2012; Li et al., 2013; Dubrulle et al., 2015; Sagner and Briscoe, 2017; Li and Elowitz, 2019; Mateus et al., 2020). In Figure 8A, we depict an example of a developing fly embryo in which a morphogen concentration increases at the anterior pole of the embryo. Over time this increase in concentration results in an increasing concentration gradient from the anterior to the posterior pole of the embryo. Cells (circle) along the embryo will experience morphogen concentration that decreases and become steeper over time (Figure 8B). However, a cell having a fixed position in the embryo will experience an increase in the morphogen concentration over time (Figure 8C). To model how cells respond to changing morphogen gradients over time, cells can be studied *in-vitro*, where the cell environment can be precisely controlled (Figure 8D).

In this review, we highlight some *in vitro* models of embryo development. For example, we choose the transforming growth factor β (TGF- β) signaling pathway as a significant pathway activated by morphogens. Further, we will focus on the ligand proteins TGF- β , bone morphogenetic proteins (BMPs), and Activin and how their gradual concentration profile that changes over time impact signaling and phenotype (Sorre et al., 2014; Heemskerk et al., 2019).

TGF- β signaling is induced by the TGF- β ligands binding to one of the five TGF- β type II receptors. TGF- β s bind the TGF- β type II receptor type 2 (TGFB2), whereas BMPs bind the BMP receptor type 2 (BMP2). These receptors are serine/threonine receptor kinases that phosphorylate one of the seven TGF- β type I receptors. A specific TGF- β type I receptor phosphorylates one of the five receptor-regulated Mothers against decapentaplegic homolog (MADs or SMADs) (R-SMAD's) (from the small worm *Caenorhabditis elegans* phenotype and MAD family of Mothers Against Decapentaplegic of genes in the fruit fly *Drosophila*). These SMADs can then bind coSMAD SMAD4. R-SMADs (SMAD1, SMAD2, SMAD3, SMAD5, SMAD9) and coSMAD can form complexes in the nucleus and act as transcription factors to regulate target genes. TGF- β signal through SMAD2 and SMAD3, whereas BMPs signal through SMAD1, SMAD5, and SMAD9. Sorre et al. (2014) showed through single-cell time-lapse microscopy experiments that acute TGF- β 1 cell stimulation (Figure 8E, black line) leads to rapid Smad4 nuclear localization followed by perfect adaptation and nuclear export (Figure 8F, black line). They then used gradual increases of TGF- β 1 (Figure 8E, colored lines) in a staircase administration and observed that Smad4 nuclear localization is rate sensitive (Figure 8F, colored lines). Interestingly, at a low rate of TGF- β 1 administration, Smad4 does not localize to the nucleus, which indicates that Smad4 nuclear localization may have a rate threshold.

Another ligand of the TGF- β pathway, BMP, also shows gradual changes over time during mouse and human development (Li et al., 2013). Li et al. (2013) observed qualitatively that BMP in mouse embryos is expressed at different locations with different TGF- β rate increases. Heemskerk et al. (2019) were interested in understanding how different BMP4 and Activin gradients that change over time regulate cell differentiation of human embryonic stem cells (hESCs). They treated these stem cells with BMP4 or Activin acutely or with linearly increasing concentrations (Figure 8E). Heemskerk et al. found that SMAD4 nuclear localization increases rapidly and adapts slowly when cells are treated with BMP4 but adapts quickly when treated with Activin (Figure 8F). However, cells respond slowly when treated with a linear increase of BMP4 or Activin. For Activin, they showed that the rate of BMP4 administration is directly proportional to the rate of SMAD4 nuclear localization. These data indicate that BMP4 and Activin administration rates can modulate SMAD4 signaling and probe a potential rate threshold in SMAD4 signaling. In future studies, one could, for example, expose these cells to different rates of TGF- β 1, Activin, and BMP4 to better understand the adaptive SMAD4 behavior, identify a potential rate threshold, and discover the proteins regulating the adaptation and rate threshold mechanisms of SMAD4 signaling.

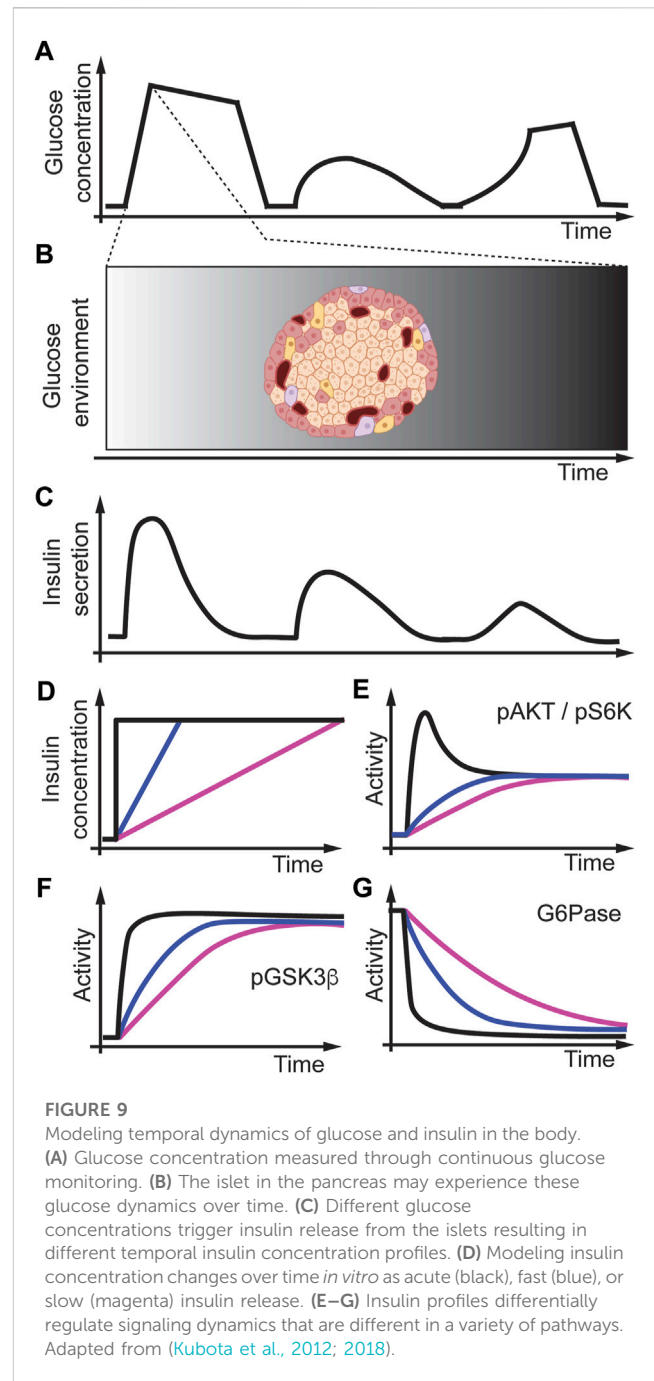
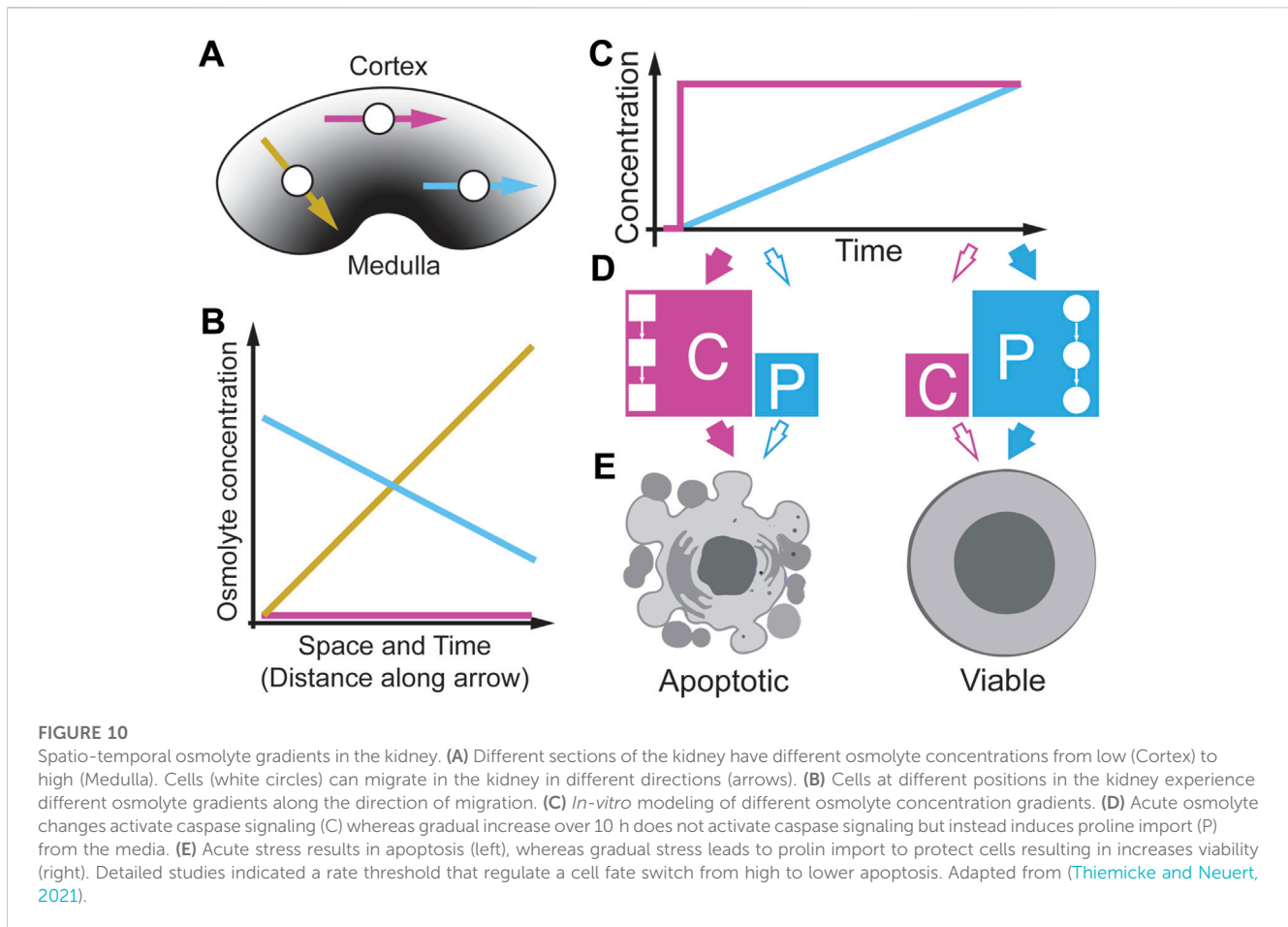


FIGURE 9

Modeling temporal dynamics of glucose and insulin in the body. (A) Glucose concentration measured through continuous glucose monitoring. (B) The islet in the pancreas may experience these glucose dynamics over time. (C) Different glucose concentrations trigger insulin release from the islets resulting in different temporal insulin concentration profiles. (D) Modeling insulin concentration changes over time *in vitro* as acute (black), fast (blue), or slow (magenta) insulin release. (E–G) Insulin profiles differentially regulate signaling dynamics that are different in a variety of pathways. Adapted from (Kubota et al., 2012; 2018).

8 Temporal dynamics of glucose and insulin signaling

A well-known example in physiology in which the concentration changes over time is the relationship between glucose uptake and insulin secretion in the body (Polonsky et al., 1988; Fernandez and Torres-Alemán, 2012). The dynamic changes in insulin secretion depend on glucose levels in the bloodstream. After a meal, glucose changes in the bloodstream in different temporal patterns as measured by continuous glucose concentration monitoring (Figure 9A). The insulin-secreting beta-cells then detect these changes in blood glucose



levels in the islets of the Langerhans in the pancreas (Figure 9B). Insulin secretion from the pancreas occurs in a pulsatile manner (Figure 9C), and this is critical to maintaining insulin receptor signaling/sensitivity (Matveyenko et al., 2012; Satin et al., 2015). Insulin secretion from the islet into the portal vein allows for higher concentrations of insulin that the liver is exposed to versus other peripheral tissues. Thus, with this high insulin concentration, the liver can undergo insulin receptor desensitization if the kinetics of insulin secretion are inappropriate. To better understand how different insulin gradients regulate cell signaling, Kubota et al. (2012) used an *in vitro* system and studied Fao rat hepatoma cells, a rat liver cell line, and exposed these cells to different acute and gradual concentrations of insulin (Figure 9D) (Noguchi et al., 2013). They then measured under these conditions, activation of the Akt pathway (Figure 9E) and downstream protein phosphorylation of glycogen synthase kinase-3b (GSK3b) (Figure 9F), gluconeogenesis through glucose-6-phosphatase (G6Pase) (Figure 9G), and phosphorylation of ribosomal protein S6 kinase (pS6) (Figure 9E) as a marker of protein synthesis. Kubota et al. (2018) then found that upon acutely increasing the concentration of insulin, the activity of pAKT, pGSK3b, and pS6K signaling proteins rapidly increases. In contrast, G6Pase activity rapidly decreases (Figures 9D–G, black lines). However, when they applied gradients of different rates of insulin to the same final concentrations,

they found that pAKT, pGSK3b, and pS6K increased slower, whereas G6Pase decreased slower, proportional to the rate of insulin increase (Figures 9D–G, colored lines). These results indicate that pAKT, pGSK3b, pS6K, and G6Pase are all rate sensitive and may encode a rate threshold. They also infused rats with acute or gradual increases in insulin through the mesenteric vein instead of into the portal vein and directly onto the liver (as it would be during islet insulin secretion). They found that in primary hepatocytes, pAKT, pGSK3b, and pS6K signaling is very similar to rat liver cell culture experiments indicating that proliferation might be rate threshold sensitive. Further studies are needed to understand better the rate threshold mechanism in cell culture and animals.

9 Temporal dynamics of stressors in the kidney

The kidney harbors one of the most extreme environments in the human body (Figure 10A) (Neuhofer and Beck, 2005; Carlström et al., 2015; Silverthorn, 2019). Of these, the inner zone is the papillary tip which regularly has the highest osmolarity levels (Figure 10A, a dark grey area) compared to the outer zone,

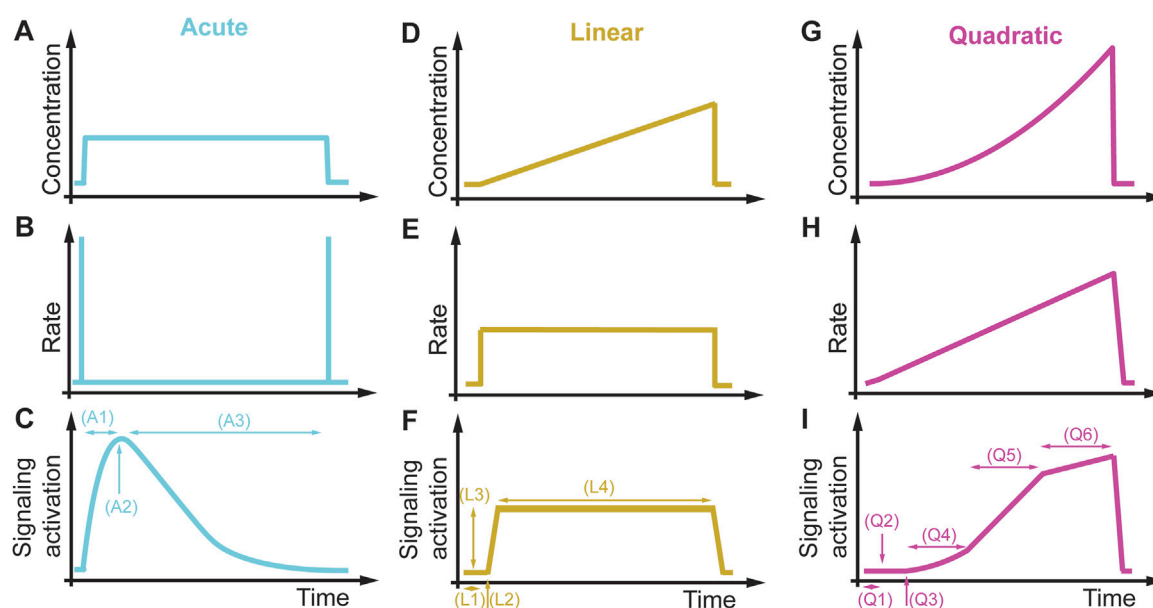


FIGURE 11

Signaling features and phenotypes in different dynamic environments. (A–C) Acute concentration changes (A) do not change the rate (B) and rapidly active signaling (C). For an adaptive pathway, acute environmental changes probe the response time of the pathway (A1), the maximum signaling response (A2), and the adaptation time (A3). (D–F) A linear concentration change (D) results in a constant rate (E), leading to prolonged signaling of an adaptive system (F). From this signaling response, we can extract the delay in signaling activation (L1), the concentration activation threshold (L2), rate-dependent signaling response amplitude (L3), and the duration and type of adaptation (L4). (G–I) Using a quadratic concentration change (G), resulting in an increasing linear rate (H) and a complex and non-linear signaling response (I). This signaling response contains information about delay in signaling activation (Q1), concentration activation threshold (Q2), rate activation threshold (Q3), linear concentration dependence (Q4), linear rate dependence (Q5), and concentration and rate saturation threshold (Q6).

named the renal medulla, which has an osmolarity level similar to plasma (Figure 10A, a light grey area). Depending on the conditions, osmolarities can at least reach 1,200 mOsmol/l in humans, four times the level found in plasma (Dantzer et al., 2014; Silverthorn, 2019). How kidney cells can survive these extreme conditions is poorly understood (Neuhofer and Beck, 2005). Interestingly, the osmolyte concentrations in the kidney change dynamically over time and follow circadian rhythms (Firsov and Bonny, 2018). If these rhythms change, they can cause several kidney pathologies, indicating that the temporal patterns of osmolyte changes may be relevant for cell survival. Surprisingly, the same cell types that can function appropriately *in vivo* die in culture when exposed to acute increases in the same osmolarity (Zhang et al., 2002; Zhang et al., 2022; Sanz et al., 2008; Thiemicke and Neuert, 2021). Further studies found that a slow increase of osmolarity drastically improves cell survival of a human kidney cell line compared to a step increase (Cai et al., 2002). A follow-up study identified gene expression differences in several osmoprotective genes as the reason for the improved survival during the gradual increase (Cai et al., 2004). They suggest that kidney cells are well-adapted to extreme hyperosmolarity. However, recent studies create an image of great cellular diversity in the kidney and show that the inner medulla and the papillary tip tissue contain immune cells (Stewart et al., 2019), indicating that immune cells in the kidney need to survive strong osmolyte gradients. An open question is how these immune cells survive in this environment

(Müller et al., 2019; Wilck et al., 2019). In Figure 10A, we depict three T cells that migrate through the kidney in different directions (Figure 10A, yellow, magenta, and cyan arrow), each experiencing different osmolyte gradients in space and time (Figure 10B). Interestingly, in pathological conditions, elevated levels of immune cells suggest that these cells survive in the kidney in this particular environment in various disease contexts (Sanz et al., 2008; Müller et al., 2019; Wilck et al., 2019). To better understand how immune cells survive in such harsh conditions, Thiemicke et al. (2019) modeled *in vitro* immune cell exposure to different osmolyte gradients (Figure 10C) and quantified cell viability as a phenotypic metric (Thiemicke and Neuert, 2021). They cultured cells in growth media and changed osmolarity by either acute or gradually increasing physiological NaCl concentrations. In T cells (Jurkat cells) and monocytes (THP1 cells), they observed that acute exposure to physiological NaCl concentrations in the kidney resulted in 85% cell death. In comparison, exposing the same cells to the same stressor and the same final concentration but at a linearly increasing concentration resulted in only 60% cell death, indicating a rate threshold in the cell viability. These results are consistent with observations in kidney cells from the Burg laboratory (Cai et al., 2002; Cai et al., 2004) and in several colon cancer cell lines (Zhang et al., 2022) confirming that elevated hypertonicity by NaCl can cause cell death. Thiemicke et al. then performed a temporal functional screen for 27 well-established markers of caspase signaling, stress signaling,

growth, inflammation, and DNA damage to identify the principal mediators of cell death. Within the markers of caspase and stress signaling, they found differential regulation of several caspases and p38 between acute and slowly increasing stress. Upon further investigation, they found that p38 signaling does not significantly contribute to the cell death phenotype. Instead, they found caspase-mediated apoptosis as the primary contributor to cell death (Figures 10D, E). Thiemicke et al. then showed through quantitative mass spectroscopy that cell internal proline increases strongly upon hypertonic stress and that proline increases to higher levels after gradual increases of hypertonic stress (Figure 10D). Supplementing external proline to Jurkat cells protects them against acutely changing stress conditions to a similar extent but synergistically when compared to caspase inhibition, demonstrating that proline functions as a molecular osmolyte similar to betaine in the kidney (Figure 10D) (Garcia-Perez and Burg, 1991; Cai et al., 2002; Burg and Ferraris, 2008). Thiemicke et al. identified differential regulation of caspase-mediated apoptosis in acute versus gradually increasing osmolyte concentration (Figure 10E). These studies suggest that proline may be used by human cells as an osmoprotective molecule, previously only described in non-human cells. The wider implications are that gradually increasing environmental changes differentially regulate human cell fate and signaling. In addition, a better understanding of how metabolic networks are coordinated with signaling networks to control cell fate may result in a novel therapeutic avenue of intervention in pathophysiological conditions.

10 Summary and future directions

The previous sections described rate dependencies of different essential signaling pathways in other organisms and suggested that these pathways may encode a rate threshold mechanism. Additional experiments must be performed at different linear or quadratic rates to test these pathways' proposed rate threshold mechanisms. From these experiments, one can learn if a pathway encodes a concentration, a rate, or both thresholds. The next step is identifying the protein(s) encoding the rate threshold. After this protein(s) has been placed, one might investigate the rate threshold mechanism through protein domain deletions, chemical inhibition, or overexpression studies. After identifying a rate threshold protein, a phenotypic assay will establish the biological relevance in different dynamic environments and rate threshold regulator mutants (see Figure 3) (Johnson et al., 2021). Besides rate thresholds, dynamic environments may also reveal other signaling features and associated phenotypes that cannot be observed in acute conditions but are relevant in non-acute physiological conditions. In Figure 11, we compare the pathway response to an acute, a linear, and a quadratic concentration change. The

acute induction (Figures 11A–C) leads to a quick increase in signaling (A1), a maximum signaling response (A2), and then a slowly decaying and adapting signaling back to the initial signaling condition (A3). In a linear increasing condition (Figures 11D–F), we can quantify the delay in signaling activation (L1), a concentration threshold (L2), a rate-dependent signaling amplitude (L3), and the duration and type of adaptation (L4).

In comparison, the same cells and pathways exposed to a quadratic increasing condition (Figures 11G–I) lead to a delay in signaling activation (Q1), a detection of a concentration activation (Q2) and rate (Q3) activation thresholds, a linear concentration (Q4) and a linear rate dependency (Q5), and a saturation concentration and rate threshold (Q6) after which signaling is not rate dependent anymore, and an increase in stimulus signal do not lead to signaling increase. This example illustrates that non-acute conditions might be vital to unraveling hidden signaling features not observable with current acute perturbation paradigms. Comparing these different signaling profiles and signaling features indicate that unique activation profiles probe special signaling features. Linking these signaling features to phenotypes and regulatory proteins will help us better understand the basic mechanisms of signal transduction in normal cells. This data and knowledge will provide the foundation to investigate how mutated signaling proteins in a pathophysiological condition alter these signaling profiles and provide the basis to develop targeted therapeutic approach. These signaling features might also be conserved or modulated throughout evolution because many of the signaling proteins are evolutionarily conserved. Quantitative data generated in these experiments will build the foundation for developing approaches for model inference, quantitative predictions, and computational screening of combinatorial protein regulation (Rahi et al., 2017; Jashnsaz et al., 2020; 2021). The proposed approaches of non-acute cell perturbations are also amenable for dissecting many other signaling processes, such as signaling cross talk, cell cycle regulation, protein translation, phase separation, and gene regulation, which are all dependent on specific signaling dynamics. Lastly, designing drug profiles in cell culture will fill a gap in understanding drug mechanisms that will guide the design of expensive and time-consuming pharmacodynamics and pharmacokinetics studies in animals and humans and improve the translatability of non-clinical studies. Finally, studying cell physiology besides the mentioned processes in non-acute conditions might reveal many hidden biological mechanisms currently not accessible with acute treatment conditions, expanding the observable phenotypic space underlying normal and pathophysiological conditions in humans as conceptualized in Figure 2.

Author contributions

GN and AT wrote the manuscript.

Funding

This work was supported by an NIH Director's New Innovator DP2 award (GM11484901), NIH R01 (GM140240), and the School of Medicine Faculty Fellow Endowed Chair to GN, and an American Heart Association (AHA) Pre-doctoral Fellowship award (18PRE34050016) to AT.

Acknowledgments

We thank P. A. Weil and D. A. Jacobson for their feedback on the manuscript.

References

- Adler, M., and Alon, U. (2018). Fold-change detection in biological systems. *Curr. Opin. Syst. Biol.* 8, 81–89. doi:10.1016/j.coisb.2017.12.005
- Alberts, B., Johnson, A., Lewis, J., Morgan, D., and Raff, M. (2015). *Molecular biology of the cell*. 6th ed. New York: Garland Science.
- Artemenko, Y., Lampert, T. J., and Devreotes, P. N. (2014). Moving towards a paradigm: Common mechanisms of chemotactic signaling in Dictyostelium and mammalian leukocytes. *Cell. Mol. Life Sci.* 71, 3711–3747. doi:10.1007/s00018-014-1638-8
- Avraham, R., and Yarden, Y. (2011). Feedback regulation of EGFR signalling: Decision making by early and delayed loops. *Nat. Rev. Mol. Cell Biol.* 12, 104–117. doi:10.1038/NRM3048
- Bandara, S., Schlöder, J. P., Eils, R., Bock, H. G., and Meyer, T. (2009). Optimal experimental design for parameter estimation of a cell signaling model. *PLoS Comput. Biol.* 5, e1000558. doi:10.1371/journal.pcbi.1000558
- Block, S. M., Segall, J. E., and Berg, H. C. (1983). Adaptation kinetics in bacterial chemotaxis. *J. Bacteriol.* 154, 312–323. doi:10.1128/jb.154.1.312-323.1983
- Block, S. M., Segall, J. E., and Berg, H. C. (1982). Impulse responses in bacterial chemotaxis. *Cell* 31, 215–226. doi:10.1016/0092-8674(82)90421-4
- Boylan, S. A., Redfield, A. R., Brody, M. S., and Price, C. W. (1993). Stress-induced activation of the sigma B transcription factor of *Bacillus subtilis*. *J. Bacteriol.* 175, 7931–7937. doi:10.1128/JB.175.24.7931-7937.1993
- Bratusch-Marrain, P. R., Komjati, M., and Waldhausl, W. K. (1986). Efficacy of pulsatile versus continuous insulin administration on hepatic glucose production and glucose utilization in type I diabetic humans. *Diabetes* 35, 922–926. doi:10.2337/DIAB.35.8.922
- Brewster, J., de Valoir, T., Dwyer, N., Winter, E., and Gustin, M. (1993). An osmosensing signal transduction pathway in yeast. *Sci.* (1979) 259, 1760–1763. doi:10.1126/science.7681220
- Brewster, J. L., and Gustin, M. C. (2014). Hog1: 20 years of discovery and impact. *Sci. Signal* 7, re7. doi:10.1126/scisignal.2005458
- Burg, M. B., and Ferraris, J. D. (2008). Intracellular organic osmolytes: Function and regulation. *J. Biol. Chem.* 283, 7309–7313. doi:10.1074/jbc.R700042200
- Cai, Q., Ferraris, J. D., and Burg, M. B. (2004). Greater tolerance of renal medullary cells for a slow increase in osmolality is associated with enhanced expression of HSP70 and other osmoprotective genes. *Am. J. Physiol. Ren. Physiol.* 286, F58–F67. doi:10.1152/ajprenal.00037.2003
- Cai, Q., Michea, L., Andrews, P., Zhang, Z., Rocha, G., Dmitrieva, N., et al. (2002). Rate of increase of osmolality determines osmotic tolerance of mouse inner medullary epithelial cells. *Am. J. Physiol. Ren. Physiol.* 283, F792–F798. doi:10.1152/ajprenal.00046.2002
- Capaldi, A. P., Kaplan, T., Liu, Y., Habib, N., Regev, A., Friedman, N., et al. (2008). Structure and function of a transcriptional network activated by the MAPK Hog1. *Nat. Genet.* 40, 1300–1306. doi:10.1038/ng.235
- Carlström, M., Wilcox, C. S., and Arendshorst, W. J. (2015). Renal autoregulation in health and disease. *Physiol. Rev.* 95, 405–511. doi:10.1152/physrev.00042.2012
- Chang, H., and Levchenko, A. (2013). Adaptive molecular networks controlling chemotactic migration: Dynamic inputs and selection of the network architecture. *Philosophical Trans. R. Soc. B Biol. Sci.* 368, 20130117. doi:10.1098/rstb.2013.0117
- Colin, R., Ni, B., Laganenka, L., and Sourjik, V. (2021). Multiple functions of flagellar motility and chemotaxis in bacterial physiology. *FEMS Microbiol. Rev.* 45, fuab038. doi:10.1093/FEMSRE/FUAB038

Conflict of interest

The authors declare that the research was conducted in the absence of any commercial or financial relationships that could be construed as a potential conflict of interest.

Publisher's note

All claims expressed in this article are solely those of the authors and do not necessarily represent those of their affiliated organizations, or those of the publisher, the editors and the reviewers. Any product that may be evaluated in this article, or claim that may be made by its manufacturer, is not guaranteed or endorsed by the publisher.

- Dantzler, W. H., Layton, A. T., Layton, H. E., and Pannabecker, T. L. (2014). Urine-concentrating mechanism in the inner medulla: Function of the thin limbs of the loops of henle. *Clin. J. Am. Soc. Nephrol.* 9, 1781–1789. doi:10.2215/CJN.08750812

- Dessaud, E., Yang, L. L., Hill, K., Cox, B., Ulloa, F., Ribeiro, A., et al. (2007). Interpretation of the sonic hedgehog morphogen gradient by a temporal adaptation mechanism. *Nature* 450 (7170), 717–720. doi:10.1038/nature06347

- Dubrulle, J., Jordan, B. M., Akhmetova, L., Farrell, J. A., Kim, S. H., Solnica-Krezel, L., et al. (2015). Response to nodal morphogen gradient is determined by the kinetics of target gene induction. *Elife* 4, e05042. doi:10.7554/eLife.05042

- English, J. G., Shellhammer, J. P., Malahe, M., McCarter, P. C., Elston, T. C., and Dohlman, H. G. (2015). MAPK feedback encodes a switch and timer for tunable stress adaptation in yeast. *Sci. Signal* 8, ra5. doi:10.1126/scisignal.2005774

- Fernandez, A. M., and Torres-Alemán, I. (2012). The many faces of insulin-like peptide signalling in the brain. *Nat. Rev. Neurosci.* 13, 225–239. doi:10.1038/nrn3209

- Ferrigno, P., Posas, F., Koepp, D., Saito, H., and Silver, P. A. (1998). Regulated nucleocytoplasmic exchange of HOG1 MAPK requires the importin beta homologs NMD5 and XPO1. *EMBO J.* 17, 5606–5614. doi:10.1093/emboj/17.19.5606

- Firsov, D., and Bonny, O. (2018). Circadian rhythms and the kidney. *Nat. Rev. Nephrol.* 14, 626–635. doi:10.1038/s41581-018-0048-9

- Fujita, K., Toyoshima, Y., Uda, S., Ozaki, Y., Kubota, H., and Kuroda, S. (2010). Decoupling of receptor and downstream signals in the Akt pathway by its low-pass filter characteristics. *Sci. Signal* 3, ra56. doi:10.1126/scisignal.2000810

- Garcia-Perez, A., and Burg, M. B. (1991). Renal medullary organic osmolytes. *Physiol. Rev.* 71, 1081–1115. doi:10.1152/physrev.1991.71.4.1081

- Gasch, A. P., Spellman, P. T., Kao, C. M., Carmel-Harel, O., Eisen, M. B., Storz, G., et al. (2000). Genomic expression programs in the response of yeast cells to environmental changes. *Mol. Biol. Cell* 11, 4241–4257. doi:10.1091/mbc.11.12.4241

- Goulev, Y., Morlot, S., Matifas, A., Huang, B., Molin, M., Toledano, M. B., et al. (2017). Nonlinear feedback drives homeostatic plasticity in H2O2 stress response. *Elife* 6, e23971–e23997. doi:10.7554/eLife.23971

- Granados, A. A., Crane, M. M., Montano-Gutierrez, L. F., Tanaka, R. J., Voliotis, M., and Swain, P. (2017). Distributing tasks via multiple input pathways increases cellular survival in stress. *Elife* 6, e21415. doi:10.7554/eLife.21415

- Gunne-Braden, A., Sullivan, A., Gharibi, B., Sheriff, R. S. M., Maity, A., Wang, Y. F., et al. (2020). GATA3 mediates a fast, irreversible commitment to BMP4-driven differentiation in human embryonic stem cells. *Cell Stem Cell* 26, 693–706. doi:10.1016/j.stem.2020.03.005

- Hashmi, A., Tlili, S., Perrin, P., Lowndes, M., Peradziryi, H., Brickman, J. M., et al. (2022). Cell-state transitions and collective cell movement generate an endoderm-like region in gastruloids. *Elife* 11, e59371. doi:10.7554/ELIFE.59371

- Hecker, M., Pané-Farré, J., and Völker, U. (2007). SigB-dependent general stress response in *Bacillus subtilis* and related gram-positive bacteria. *Annu. Rev. Microbiol.* 61, 215–236. doi:10.1146/ANNUREV.MICRO.61.080706.093445

- Heemskerk, I., Burt, K., Miller, M., Chhabra, S., Guerra, M. C., Liu, L., et al. (2019). Rapid changes in morphogen concentration control self-organized patterning in human embryonic stem cells. *Elife* 8, e40526. doi:10.7554/eLife.40526

- Hersen, P., McClean, M. N., Mahadevan, L., and Ramanathan, S. (2008). Signal processing by the HOG MAP kinase pathway. *PNAS* 105, 7165–7170. doi:10.1073/pnas.0710770105

- Hill, C. S. (2018). Spatial and temporal control of NODAL signaling. *Curr. Opin. Cell Biol.* 51, 50–57. doi:10.1016/j.cceb.2017.10.005
- Jacoby, T., Flanagan, H., Faykin, A., Seto, A. G., Mattison, C., and Ota, I. (1997). Two protein-tyrosine phosphatases inactivate the osmotic stress response pathway in yeast by targeting the mitogen-activated protein kinase, Hog1. *J. Biol. Chem.* 272, 17749–17755. doi:10.1074/jbc.272.28.17749
- Jashnsaz, H., Fox, Z. R., Hughes, J., Li, G., Munsky, B. E., and Neuert, G. (2020). Diverse cell stimulation kinetics identify predictive signal transduction models. *iScience* 23, 101565. doi:10.1016/j.isci.2020.101565
- Jashnsaz, H., Fox, Z. R., Munsky, B., Neuert, G., Fox, R. Z., Munsky, B., et al. (2021). Building predictive signaling models by perturbing yeast cells with time-varying stimulations resulting in distinct signaling responses. *Star. Protoc.* 2, 100660. doi:10.1016/j.xpro.2021.100660
- Ji, Y., Lu, Y., Yang, F., Shen, W., Tang, T. T., Feng, L., et al. (2010). Acute and gradual increases in BDNF concentration elicit distinct signaling and functions in neurons. *Nat. Neurosci.* 13, 302–309. doi:10.1038/NN.2505
- Johnson, A. N., Li, G., Jashnsaz, H., Thiemicke, A., Kesler, B. K., Rogers, D. C., et al. (2021). A rate threshold mechanism regulates MAPK stress signaling and survival. *PNAS* 118, e2004998118. doi:10.1073/pnas.2004998118
- Karmakar, R. (2021). State of the art of bacterial chemotaxis. *J. Basic Microbiol.* 61, 366–379. doi:10.1002/JOBM.202000661
- Keestra, J. M., Carrara, F., and Stocker, R. (2022). The ecological roles of bacterial chemotaxis. *Nat. Rev. Microbiol.* 20, 491–504. doi:10.1038/S41579-022-00709-W
- Koseska, A., and Bastiaens, P. I. H. (2020). Processing temporal growth factor patterns by an epidermal growth factor receptor network dynamically established in space. *Annu. Rev. Cell Dev. Biol.* 36, 359–383. doi:10.1146/ANNUREV-CELLBIO-013020-103810
- Krause, H. B., Bondarowicz, H., Karls, A. L., McClean, M. N., and Kreeger, P. K. (2021). Design and implementation of a microfluidic device capable of temporal growth factor delivery reveal filtering capabilities of the EGFR/ERK pathway. *Apl. Bioeng.* 5, 046101. doi:10.1063/5.0059011
- Kubota, H., Noguchi, R., Toyoshima, Y., Ozaki, Y., Uda, S., Watanabe, K., et al. (2012). Temporal coding of insulin action through multiplexing of the AKT pathway. *Mol. Cell* 46, 820–832. doi:10.1016/j.molcel.2012.04.018
- Kubota, H., Uda, S., Matsuzaki, F., Yamauchi, Y., and Kuroda, S. (2018). *In vivo* decoding mechanisms of the temporal patterns of blood insulin by the insulin-AKT pathway in the liver. *Cell Syst.* 7, 118–128. doi:10.1016/j.cels.2018.05.013
- Kutejova, E., Briscoe, J., and Kicheva, A. (2009). Temporal dynamics of patterning by morphogen gradients. *Curr. Opin. Genet. Dev.* 19, 315–322. doi:10.1016/J.GDE.2009.05.004
- Li, L., Liu, C., Biechele, S., Zhu, Q., Song, L., Lanner, F., et al. (2013). Location of transient ectodermal progenitor potential in mouse development. *Development* 140, 4533–4543. doi:10.1242/DEV.092866
- Li, P., and Elowitz, M. B. (2019). Communication codes in developmental signaling pathways. *Development* 146, dev170977. doi:10.1242/dev.170977
- Lim, W., Mayer, B., and Pawson, T. (2014). *Cell signaling: Principles and mechanisms*. 1st ed. New York, USA: Garland Science, Taylor and Francis Group, LLC. 978-0-8153-4244-1.
- Luecke, S., Sheu, K. M., and Hoffmann, A. (2021). Stimulus-specific responses in innate immunity: Multilayered regulatory circuits. *Immunity* 54, 1915–1932. doi:10.1016/J.IMMUNI.2021.08.018
- Ma, W., Trusina, A., El-Samad, H., Lim, W. A., and Tang, C. (2009). Defining network topologies that can achieve biochemical adaptation. *Cell* 138, 760–773. doi:10.1016/j.cell.2009.06.013
- Macia, J., Regot, S., Peeters, T., Conde, N., Solé, R., Posas, F., et al. (2009). Dynamic signaling in the Hog1 MAPK pathway relies on high basal signal transduction. *Sci. Signal* 2, ra13. doi:10.1126/scisignal.2000056
- Maeda, T., Wurgler-Murphy, S. M., and Saito, H. (1994). A two-component system that regulates an osmosensing MAP kinase cascade in yeast. *Nature* 369, 242–245. doi:10.1038/369242a0
- Mapes, J., and Ota, I. M. (2004). Nbp2 targets the Ptc1-type 2C Ser/Thr phosphatase to the HOG MAPK pathway. *EMBO J.* 23, 302–311. doi:10.1038/sj.emboj.7600036
- Mateus, R., Holtzer, L., Seum, C., Hadjivasilou, Z., Dubois, M., Jülicher, F., et al. (2020). BMP signaling gradient scaling in the zebrafish pectoral fin. *Cell Rep.* 30, 4292–4302. doi:10.1016/j.celrep.2020.03.024
- Mattison, C. P., and Ota, I. M. (2000). Two protein tyrosine phosphatases, Ptp2 and Ptp3, modulate the subcellular localization of the Hog1 MAP kinase in yeast. *Genes Dev.* 14, 1229–1235. doi:10.1101/gad.14.10.1229
- Matveyenko, A. v., Liuwantara, D., Gurlo, T., Kirakossian, D., Dalla Man, C., Cobelli, C., et al. (2012). Pulsatile portal vein insulin delivery enhances hepatic insulin action and signaling. *Diabetes* 61, 2269–2279. doi:10.2337/DB11-1462
- Meizlish, M. L., Franklin, R. A., Zhou, X., and Medzhitov, R. (2021). Tissue homeostasis and inflammation. *Annu. Rev. Immunol.* 39, 557–581. doi:10.1146/ANNUREV-IMMUNOL-061020-053734
- Mettetal, J. T., Muzzey, D., Gómez-Urbe, C., van Oudenaarden, A., Gomez-Urbe, C., van Oudenaarden, A., et al. (2008). The frequency dependence of osmo-adaptation in *Saccharomyces cerevisiae*. *Sci.* (1979) 319, 482–484. doi:10.1126/science.1151582
- Milo, R., Shen-Orr, S., Itzkovitz, S., Kashtan, N., Chklovskii, D., and Alon, U. (2002). Network motifs: Simple building blocks of complex networks. *Sci.* (1979) 298, 824–827. doi:10.1126/science.298.5594.824
- Mitchell, A., Wei, P., and Lim, W. A. (2015). Oscillatory stress stimulation uncovers an Achilles heel of the yeast MAPK signaling network. *Sci.* (1979) 350, 1379–1383. doi:10.1126/science.aab0892
- Mokashi, C. S., Schipper, D. L., Qasaimeh, M. A., and Lee, R. E. C. (2019). A System for analog control of cell culture dynamics to reveal capabilities of signaling networks. *iScience* 19, 586–596. doi:10.1016/j.isci.2019.08.010
- Müller, D. N., Wilck, N., Haase, S., Kleinewietfeld, M., and Linker, R. A. (2019). Sodium in the microenvironment regulates immune responses and tissue homeostasis. *Nat. Rev. Immunol.* 19, 243–254. doi:10.1038/s41577-018-0113-4
- Munsky, B., Neuert, G., and van Oudenaarden, A. (2012). Using gene expression noise to understand gene regulation. *Sci.* (1979) 336, 183–187. doi:10.1126/science.1216379
- Murugan, A., Husain, K., Rust, M. J., Hepler, C., Bass, J., Pietsch, J. M. J., et al. (2021). Roadmap on biology in time varying environments. *Phys. Biol.* 18, 041502. doi:10.1088/1478-3975/ABDE8D
- Muzzey, D., Gómez-Urbe, C. A., Mettetal, J. T., and van Oudenaarden, A. (2009). A systems-level analysis of perfect adaptation in yeast osmoregulation. *Cell* 138, 160–171. doi:10.1016/j.cell.2009.04.047
- Nadal-Ribelles, M., Solé, C., Xu, Z., Steinmetz, L. M., de Nadal, E., and Posas, F. (2014). Control of Cdc28 CDK1 by a stress-induced lncRNA. *Mol. Cell* 53, 549–561. doi:10.1016/j.molcel.2014.01.006
- Neuert, G., Munsky, B., Tan, R. Z., Teytelman, L., Khammash, M., and van Oudenaarden, A. (2013). Systematic identification of signal-activated stochastic gene regulation. *Sci.* (1979) 339, 584–587. doi:10.1126/science.1231456
- Neuhof, W., and Beck, F.-X. (2005). Cell Survival in the hostile environment of the renal medulla. *Annu. Rev. Physiol.* 67, 531–555. doi:10.1146/annurev.physiol.67.031103.154456
- Nguyen-Huu, T. D., Gupta, C., Ma, B., Ott, W., Josić, K., and Bennett, M. R. (2015). Timing and variability of galactose metabolic gene activation depend on the rate of environmental change. *PLoS Comput. Biol.* 11, e1004399. doi:10.1371/JOURNAL.PCBL1004399
- Nichols, J. M. E., Veltman, D., and Kay, R. R. (2015). Chemotaxis of a model organism: Progress with Dictyostelium. *Curr. Opin. Cell Biol.* 36, 7–12. doi:10.1016/J.CEB.2015.06.005
- Noguchi, R., Kubota, H., Yugi, K., Toyoshima, Y., Komori, Y., Soga, T., et al. (2013). The selective control of glycolysis, gluconeogenesis and glycogenesis by temporal insulin patterns. *Mol. Syst. Biol.* 9, 664. doi:10.1038/msb.2013.19
- Park, H., and Poo, M. M. (2012). Neurotrophin regulation of neural circuit development and function. *Nat. Rev. Neurosci.* 14 (1 14), 7–23. doi:10.1038/nrn3379
- Patterson, J. C., Klimenko, E. S., and Thorner, J. (2010). Single-cell analysis reveals that insulation maintains signaling specificity between two yeast MAPK pathways with common Components. *Sci. Signal* 3, ra75. ARTN. doi:10.1126/scisignal.2001275
- Pelet, S., Rudolf, F., Nadal-Ribelles, M., de Nadal, E., Posas, F., and Peter, M. (2011). Transient activation of the HOG MAPK pathway regulates bimodal gene expression. *Sci.* (1979) 332, 732–735. doi:10.1126/science.1198851
- Polonsky, K. S., Given, B. D., and Van Cauter, E. (1988). Twenty-four-hour profiles and pulsatile patterns of insulin secretion in normal and obese subjects. *J. Clin. Invest.* 81, 442–448. doi:10.1172/JCI113339
- Posas, F., and Saito, H. (1997). Osmotic activation of the HOG MAPK pathway via Ste11p MAPKKK: Scaffold role of Pbs2p MAPKK. *Science* 276, 1702–1705. doi:10.1126/science.276.5319.1702
- Posas, F., Wurgler-Murphy, S. M., Maeda, T., Witten, E. A., Thai, T. C., and Saito, H. (1996). Yeast HOG1 MAP kinase cascade is regulated by a multistep phosphorylation mechanism in the SLN1-YPD1-SSK1 “two-component” osmosensor. *Cell* 86, 865–875. doi:10.1016/S0092-8674(00)80162-2
- Rahi, S. J., Larsch, J., Pecani, K., Katsov, A. Y., Mansouri, N., Tsaneva-Atanasova, K., et al. (2017). Oscillatory stimuli differentially adapting circuit topologies. *Nat. Methods* 14, 1010–1016. doi:10.1038/nmeth.4408
- Reiser, V., Ruis, H., and Ammerer, G. (1999). Kinase activity-dependent nuclear export opposes stress-induced nuclear accumulation and retention of Hog1 mitogen-activated protein kinase in the budding yeast *Saccharomyces cerevisiae*. *Mol. Biol. Cell* 10, 1147–1161. doi:10.1091/mbc.10.4.1147
- Rep, M., Krantz, M., Thevelein, J. M., and Hohmann, S. (2000). The Transcriptional Response of *Saccharomyces cerevisiae* to Osmotic Shock. Hot1p and Msn2p/Msn4p are required for the induction of subsets of high osmolarity glycerol pathway-dependent genes. *J. Biol. Chem.* 275, 8290–8300. doi:10.1074/jbc.275.12.8290
- Rushlow, C. A., and Shvartsman, S. Y. (2012). Temporal dynamics, spatial range, and transcriptional interpretation of the Dorsal morphogen gradient. *Curr. Opin. Genet. Dev.* 22, 542–546. doi:10.1016/j.gde.2012.08.005

- Sagner, A., and Briscoe, J. (2017). Morphogen interpretation: Concentration, time, competence, and signaling dynamics. *Wiley Interdiscip. Rev. Dev. Biol.* 6 (4), e271. doi:10.1002/wdev.271
- Saito, H., and Posas, F. (2012). Response to hyperosmotic stress. *Genetics* 192, 289–318. doi:10.1534/genetics.112.140863
- Sano, T., Kawata, K., Ohno, S., Yugi, K., Kakuda, H., Kubota, H., et al. (2016). Selective control of up-regulated and down-regulated genes by temporal patterns and doses of insulin. *Sci. Signal* 9, ra112. doi:10.1126/scisignal.aaf3739
- Sanz, A. B., Santamaría, B., Ruiz-Ortega, M., Egido, J., and Ortiz, A. (2008). Mechanisms of renal apoptosis in health and disease. *J. Am. Soc. Nephrol.* 19, 1634–1642. doi:10.1681/ASN.2007121336
- Sasagawa, S., Ozaki, Y., Fujita, K., and Kuroda, S. (2005). Prediction and validation of the distinct dynamics of transient and sustained ERK activation. *Nat. Cell Biol.* 7, 365–373. doi:10.1038/ncb1233
- Satin, L. S., Butler, P. C., Ha, J., and Sherman, A. S. (2015). Pulsatile insulin secretion, impaired glucose tolerance and type 2 diabetes. *Mol. Asp. Med.* 42, 61–77. doi:10.1016/j.MAM.2015.01.003
- Segall, J. E., Block, S. M., and Berg, H. C. (1986). Temporal comparisons in bacterial chemotaxis. *Proc. Natl. Acad. Sci. U. S. A.* 83, 8987–8991. doi:10.1073/PNAS.83.23.8987
- Sgro, A. E., Schwab, D. J., Noorbakhsh, J., Mestler, T., Mehta, P., and Gregor, T. (2015). From intracellular signaling to population oscillations: Bridging size- and time-scales in collective behavior. *Mol. Syst. Biol.* 11, 779. doi:10.15252/MSB.20145352
- Shimizu, T. S., Tu, Y., and Berg, H. C. (2010). A modular gradient-sensing network for chemotaxis in *Escherichia coli* revealed by responses to time-varying stimuli. *Mol. Syst. Biol.* 6, 382. doi:10.1038/msb.2010.37
- Silverthorn, D. U. (2019). in *Human physiology - an integrated approach*. Editors B. R. Johnson, W. C. Ober, C. E. Ober, A. Impaglizzo, and A. C. Silverthorn 8th ed. (London, United Kingdom: Pearson).
- Sorre, B., Warmflash, A., Brivanlou, A. H., and Siggia, E. D. (2014). Encoding of temporal signals by the TGF- β Pathway and implications for embryonic patterning. *Dev. Cell* 30, 334–342. doi:10.1016/j.devcel.2014.05.022
- Stanger, K., Gorelik, M., and Davidson, A. R. (2012). Yeast adaptor protein, Nbp2p, is conserved regulator of fungal Ptc1p phosphatases and is involved in multiple signaling pathways. *J. Biol. Chem.* 287, 22133–22141. doi:10.1074/JBC.M112.348052
- Stelling, J., Sauer, U., Szallasi, Z., Doyle, F. J., III, and Doyle, J. (2004). Robustness of cellular functions. *Cell* 118, 675–685. doi:10.1016/j.cell.2004.09.008
- Stewart, B. J., Ferdinand, J. R., Young, M. D., Mitchell, T. J., Loudon, K. W., Riding, A. M., et al. (2019). Spatiotemporal immune zonation of the human kidney. *Science* 365, 1461–1466. doi:10.1126/science.aat5031
- Tewary, M., Ostblom, J., Prochazka, L., Zulueta-Coarasa, T., Shakiba, N., Fernandez-Gonzalez, R., et al. (2017). A stepwise model of reaction-diffusion and positional information governs self-organized human peri-gastrulation-like patterning. *Development* 144, 4298–4312. doi:10.1242/DEV.149658
- Thiemicke, A., Jashnsaz, H., Li, G., and Neuert, G. (2019). Generating kinetic environments to study dynamic cellular processes in single cells. *Sci. Rep.* 9, 10129. doi:10.1038/s41598-019-46438-8
- Thiemicke, A., and Neuert, G. (2021). Kinetics of osmotic stress regulate a cell fate switch of cell survival. *Sci. Adv.* 7 (8), eabe1122. doi:10.1126/sciadv.abe1122
- Tu, Y., and Rappel, W.-J. J. (2018). Adaptation of living systems. *Annu. Rev. Condens Matter Phys.* 9, 183–205. doi:10.1146/annurev-conmatphys-033117-054046
- Tu, Y., Shimizu, T. S., and Berg, H. C. (2008). Modeling the chemotactic response of *Escherichia coli* to time-varying stimuli. *Proc. Natl. Acad. Sci. U. S. A.* 105, 14855–14860. doi:10.1073/pnas.0807569105
- Waite, A. J., Frankel, N. W., and Emonet, T. (2018). Behavioral variability and phenotypic diversity in bacterial chemotaxis. *Annu. Rev. Biophys.* 47, 595–616. doi:10.1146/ANNUREV-BIOPHYS-062215-010954
- Wang, C. J., Bergmann, A., Lin, B., Kim, K., and Levchenko, A. (2012). Diverse sensitivity thresholds in dynamic signaling responses by social Amoebae. *Sci. Signal* 5, ra17. doi:10.1126/scisignal.2002449
- Wang, C. S., Kavalali, E. T., and Monteggia, L. M. (2022). BDNF signaling in context: From synaptic regulation to psychiatric disorders. *Cell* 185, 62–76. doi:10.1016/j.CELL.2021.12.003
- Warmka, J., Hanneman, J., Lee, J., Amin, D., and Ota, I. (2001). Ptc1, a type 2C ser/thr phosphatase, inactivates the HOG pathway by dephosphorylating the mitogen-activated protein kinase Hog1. *Mol. Cell Biol.* 21, 51–60. doi:10.1128/mcb.21.1.51-60.2001
- Westfall, P. J., and Thorner, J. (2006). Analysis of mitogen-activated protein kinase signaling specificity in response to hyperosmotic stress: Use of an analog-sensitive HOG1 allele. *Eukaryot. Cell* 5, 1215–1228. doi:10.1128/EC.00037-06
- Wilck, N., Balogh, A., Markó, L., Bartolomaeus, H., and Müller, D. N. (2019). The role of sodium in modulating immune cell function. *Nat. Rev. Nephrol.* 15, 546–558. doi:10.1038/s41581-019-0167-y
- Wurgler-Murphy, S. M., Maeda, T., Witten, E. A., and Saito, H. (1997). Regulation of the *Saccharomyces cerevisiae* HOG1 mitogen-activated protein kinase by the PTP2 and PTP3 protein tyrosine phosphatases. *Mol. Cell Biol.* 17, 1289–1297. doi:10.1128/MCB.17.3.1289
- Young, C., Mapes, J., Hanneman, J., Al-Zarban, S., and Ota, I. (2002). Role of Ptc2 type 2C Ser/Thr phosphatase in yeast high-osmolarity glycerol pathway inactivation. *Eukaryot. Cell* 1, 1032–1040. doi:10.1128/EC.1.6.1032-1040.2002
- Young, J. W., Locke, J. C. W., and Elowitz, M. B. (2013). Rate of environmental change determines stress response specificity. *Proc. Natl. Acad. Sci. U. S. A.* 110, 4140–4145. doi:10.1073/pnas.1213060110
- Zhang, W., Fan, W., Guo, J., and Wang, X. (2022). Osmotic stress activates RIPK3/MLKL-mediated necroptosis by increasing cytosolic pH through a plasma membrane Na⁺/H⁺-exchanger. *Sci. Signal* 15, 5881. doi:10.1126/scisignal.abn5881
- Zhang, Z., Cai, Q., Michea, L., Dmitrieva, N. I., Andrews, P., and Burg, M. B. (2002). Proliferation and osmotic tolerance of renal inner medullary epithelial cells *in vivo* and in cell culture. *Am. J. Physiol. Ren. Physiol.* 283 (2), F302–F308. doi:10.1152/ajprenal.00038.2002